THE INFRA-RED AND ULTRAVIOLET SPECTRA OF PROPYNAL

by

DAVID CECIL MOULE, B.Sc.

A Thesis

Submitted to the Faculty of Graduate Studies

in Partial Fulfillment of the Requirements

for the Degree

Doctor of Philosophy

McMaster University

October 1962

DOCTOR OF PHILOSOPHY (1962)
(Chemistry)

McMASTER UNIVERSITY
Hamilton, Ontario

TITLE: The Infra-red and Ultraviolet Spectra of Propynal

AUTHOR: David Cecil Moule, B.Sc. (McMaster University)

SUPERVISOR: Dr. G. W. King

NUMBER OF PAGES 107, vi

SCOPE AND CONTENTS:

The infra-red spectra of gaseous HC≡CCHO, DC≡CCHO, HC≡CCDO and the Raman spectrum of liquid HC≡CCHO has been measured and analysed to give the normal vibrational frequencies of the molecule in the electronic ground state. The electronic band spectrum of propynal with origin at 4144 Å has been photographed under low resolution in both emission and absorption and analysed in terms of the vibrational frequencies associated with the combining electronic states. The origin band for both HC≡CCHO and DC≡CCHO has been photographed under high resolution and a partial rotational analysis is presented for this band. The transition responsible for the electronic spectrum has been identified as being of $n \longrightarrow {}^3\pi^*$, ${}^3A'' \longleftarrow {}^1A'$ type, and the observed spectrum confirms the theoretical predictions as to the structure that results from a transition of this type.

ACKNOWLEDGEMENTS

I am very grateful to Dr. G. W. King for his advice and encouragement during my research work and thesis preparation.

I also wish to thank the following people for their generous assistance: Dr. J. C. D. Brand for allowing me to read his unpublished work on propynal, Dr. C. C. Costain for donating the HC≡CCDO, Dr. R. H. Tomlinson for donating a sample of D_2O, and Dr. R. J. Gillespie for the use of the Raman Spectrograph. I also wish to acknowledge the stimulus provided by my colleagues, R. D. Gordon, J. L. Hencher, V. A. Job, G. L. Malli and A. W. Richardson.

The assistance provided by Miss Susan Notman in the preparation and typing of this thesis has been invaluable.

Finally I should like to thank the Department of Chemistry for granting me a scholarship for 1958-1959. Thanks are also due to Dow Chemical Company for granting me a scholarship for 1959-1960 and Canadian Industries Limited for 1960-1962.

TABLE OF CONTENTS

LIST OF TABLES

LIST OF FIGURES

THE INFRA-RED AND ULTRAVIOLET SPECTRA OF PROPYNAL

^{14}C

CHAPTER 1.

INTRODUCTION

In the quantum mechanical picture, the Hamiltonian operator H corresponding to the internal energy of a molecule has eigenvalues E, and eigenfunctions Ψ that satisfy the wave equation

$$H\Psi = E\Psi \tag{1.1}$$

The Born-Oppenheimer approximation states that the total energy E can be decomposed into separate contributions due to the electronic and nuclear motions; and to a first approximation, the nuclear energy can be taken as the sum of separately quantised components due to vibrational and rotational motion. So the total energy (apart from that ascribed to electron and nuclear spin) can be written

$$E = E_e + E_v + E_r \tag{1.2}$$

and correspondingly, the total wavefunction may be factored into a product of associated wavefunctions

$$\Psi = \Psi_e \Psi_v \Psi_r \tag{1.3}$$

with

$$H = H_e + H_v + H_r \tag{1.4}$$

There follows from this approximation the useful result that the quantum mechanical description for each of the vibrational,

rotational and electronic motions of the molecule may be treated independently, since we may write

$$H_e \Psi_e = E_e \Psi_e \tag{1.5a}$$

$$H_v \Psi_v = E_v \Psi_v \tag{1.5b}$$

$$H_r \Psi_r = E_r \Psi_r \tag{1.5c}$$

When a transition occurs from one state Ψ' of a molecule to another Ψ'' with the absorption or emission of energy as radiation, the resulting spectrum will consist of a spectral line of wave-number (cm-1)

$$\nu = \frac{E' - E''}{hc} \tag{1.6}$$

where E' and E" are the energies of upper and lower states, h is Planck's constant and c the velocity of light.

The probability of such a transition occurring between two states with wave functions Ψ' and Ψ'' is determined to a first approximation by the square of the matrix elements.

$$R_x = \int \Psi' \mu_x \Psi'' \, d_x \tag{1.7a}$$

$$R_y = \int \Psi' \mu_y \Psi'' \, d_y \tag{1.7b}$$

$$R_z = \int \Psi' \mu_z \Psi'' \, d_z \tag{1.7c}$$

R_x, R_y and R_z are the components of the transition moment, and μ_x, μ_y, μ_z are the components of the electric dipole moment along three mutually perpendicular axes x, y, and z. For a finite transition probability, at least one of the components of the transition moment must have a non-zero value. Group theoretical methods can be applied to the factors in the integrands in equation (1.5) to establish whether or not the integrals will vanish.

If one of the integrals has a non-zero value, the transition moment will be finite and the transition is allowed as an electric dipole transition. If all components of the transition moment are equal to zero the transition is forbidden.

Because of the relatively small energy separation between rotational energy levels E_r, transitions which only involve a change in the rotational quantum number produce spectra in the microwave region (0.1 - 10 cm^{-1}). Changes in vibrational energy E_v give bands in the infra-red region (200 - 4000 cm^{-1}). Each of these bands consists of rotational fine structure due to transitions between the rotational energy levels accompanying each vibrational level. The electronic band spectra of a molecule, which correspond to transitions between one electronic state and another are generally observed in the visible and ultra-violet regions, (10,000 - 100,000 cm^{-1}). Each electronic spectrum consists of a series of bands, due to transitions between vibrational energy levels, in the combining electronic states, and each band in turn displays a rotational fine structure. An analysis of an electronic band spectrum provides details of the geometric and elastic properties of the two combining electronic states.

During recent years, considerable effort has been devoted to the detailed study of electronic band spectra of simple poly-atomic molecules. The rapid development of this subject can be seen from the following chronological list of molecules, ions and free radicals for which rotational analysis have been carried out.

Prior to 1940	H_2CO, CO_2
1940 - 1950	CS_2, CO_2^+, SO_2, NO_2, ClO_2
1950 - 1960	C_2H_2, HCN, CS_2, H_2CO, $(HCO)_2$
	CS_2^+, $C_2H_2^+$, NH_2, HCO, CH_3, HNO
1960 - 1961	NO_2, HCOF, C_6H_6, $C_{10}H_8$, NH_3, CH_2, BO_2

There is, therefore, available at the present time a fairly detailed knowledge of these species in their ground and excited electronic states.

Before such an analysis can be made on a polyatomic molecule, a number of definite requirements must be satisfied.

(a) The main requirement is, of course, that the molecule must absorb or emit in an experimentally accessible region. For studies in the visible or near ultra-violet, the molecule must contain multiple bonds, or it must have non-bonding orbitals adjacent to multiple bonds.

(b) The band spectrum of the molecule must have a discrete vibrational and rotational structure. This criterion is difficult to predict in advance since the bands may be diffuse because of the occurrence of dissociation or predissociation in the electronically excited state.

(c) The moments of inertia of the molecule must be sufficiently small to enable the rotational structure of the bands to be resolved experimentally with the spectroscopic apparatus available.

For molecules with molecular weights in the range 50 - 100 an instrumental resolving power of at least 150,000 is usually necessary. If two of the three principal moments of inertia are equal, the rotational structure of the bands is simplified.

(d) It is preferable that the molecule should contain relatively few atoms to ensure that the number of vibrational degrees of freedom is small, or a high symmetry to limit the number of vibrations that are active in the spectra. Otherwise overlapping of the bands may cause uncertainties in the analysis when the resolving power of the spectrograph is limited.

(e) The possibility of obtaining isotopically substituted compounds is also a factor to consider, since when the spectra of a number of isotopic species are available the vibrational and rotational analyses, and the determination of the molecular geometry are facilitated.

Propynal HC≡CCHO, which is the simplest combination of the acetylenic and aldehydic groups makes an interesting study from a spectroscopic point of view, since it satisfies most of the above requirements.

Recently, two microwave studies have been made on propynal. Howe and Goldstein[1] studied rotational transitions in the ground

vibronic state of the naturally abundant isomer and concluded that the molecule was a planar near-prolate symmetric top. They were able to define the molecular geometry only approximately, since only transitions directed along the a and b principal axes were observed. In 1959 Costain and Morton[2] were able to determine accurately the bond angles and bond lengths of propynal from a rotational analysis of the microwave spectra of 15 isotopic species.

The ultra-violet absorption spectrum was examined under medium resolution by Howe and Goldstein[3]. Besides observing diffuse absorption in the 2000 Å region, they found that between 3000-4000 Å a large number of sharp vibrational bands appeared with low intensity. From a partial vibrational analysis of these bands, they concluded that the origin of the system was at 3820 Å and a transition to the lowest singlet electronically excited state was responsible, in which an electron is promoted from a non-bonding orbital on the oxygen atom into an anti-bonding orbital in the carbonyl group.

CHAPTER 2

THEORY OF THE INFRA-RED SPECTRA

I. MOLECULAR VIBRATIONS: In order to analyse the nuclear motions of a polyatomic molecule, each of the N atoms is regarded as a point mass. A total of 3N coordinates is necessary to describe the displacements of the atoms when the molecule is in motion, these could be, for example, the Cartesian components x_i, y_i and z_i measuring the displacement of each atom from its rest position. We shall represent displacements by the generalised set of coordinates $q_1 \ldots q_{3N}$. If the atoms are constrained to move so that there is no resultant linear or angular momentum for the molecule as a whole, that is, it executes vibrational but not rotational or translational motions, then six of these coordinates are redundant, a non-linear molecule having only 3N-6 vibrational degrees of freedom.

The potential energy V of the system may be represented by a Taylor series expansion when the displacements q_i are small

$$V = V_o + \tfrac{1}{2} \sum_{i=1}^{3N} \left(\frac{\partial V}{\partial q_i}\right)_o q_i + \tfrac{1}{2} \sum_{i,j=1}^{3N} \left(\frac{\partial^2 V}{\partial q_i \partial q_j}\right) q_i q_j + \ldots \quad (2.1)$$

V_o is the potential energy of the nuclei in their equilibrium configuration and can be set equal to zero. The second term in the expansion is also zero, since V is a minimum for the equilibrium configuration. The quadratic term remaining in (2.1) represents the potential energy for small atomic displacements, and may be written

$$V = \tfrac{1}{2} \sum_{i,j=1}^{3N} f_{ij} q_j q_i \qquad (2.2)$$

where f_{ij} are constant for a given molecule. The kinetic energy of the system is

$$T = \tfrac{1}{2} \Sigma_i m_i \dot{q}_i^2 \qquad (2.3)$$

By means of an orthogonal transformation upon the generalised co-ordinates q_i, of type

$$Q_i = \Sigma_{ij} a_{ij} q_i \qquad (2.4)$$

it is possible to transfer to a coordinate system $Q_1 \ldots Q_{3N}$, in which the potential energy has the simple form

$$V = \tfrac{1}{2} \sum_{i=1}^{3N} f'_i Q_i^2 \qquad (2.5)$$

also the kinetic energy is

$$T = \tfrac{1}{2} \sum_{i=1}^{3N} m_i \dot{Q}_i^2 \qquad (2.6)$$

The Q_i are called the normal coordinates of the system, and with their use the equations of motion are reduced to their simplest form. Thus when T and V are replaced by their corresponding operators in the vibrational wave equation, the latter can be reduced to

$$\sum_{i=1}^{3N} \frac{\partial^2 \psi}{\partial Q_i^2} + \frac{8\pi^2}{h^2} \left(E_v - \sum_{i=1}^{3N} \frac{f'_i Q_i^2}{2m_i}\right) \psi = 0$$

which, upon separation of the variables by substituting

$$\psi = \psi_1 (Q_1) \psi_2 (Q_2) \ldots \psi_{3N} (Q_{3N}) \qquad (2.8)$$

resolves into 3N equations, each of form

$$\frac{d^2 \psi_i (Q_i)}{dQ_i^2} + \frac{8\pi^2}{h^2} \left(E_i - \frac{f'_i Q_i^2}{2m_i}\right) \psi_i (Q_i) = 0$$

where

$$E = \sum_i E_i \qquad (2.10$$

Each of the equations (2.9) has the form of a wave equation for a simple harmonic oscillator, and has eigenvalues

$$E_i(v_i) = (v_i + \tfrac{1}{2})h\nu_i^\circ$$

where v_i is vibrational quantum number and ν_i° is the classical frequency of vibration. (Six of the equations, however, correspond to the three rotational and three translational degrees of freedom for the non-linear molecule, which have zero frequency; the remaining 3N-6 equations represent genuine vibrations). In terms of normal coordinates, therefore, the vibrational motion of the molecule can be analysed into 3N-6 independent vibrational modes, each of these being directed along a normal coordinate.

II. SYMMETRY: Solution of the vibrational wave equation to obtain the eigenvalues and eigenfunctions for a polyatomic molecule represents a tedious calculation, although electronic computers are widely used nowadays to accelerate the process. Many properties of the normal vibrations, and also the selection rules for spectroscopic transitions, may be determined without detailed calculation when use is made of the symmetry properties of molecules.

The nuclear framework of a molecule in its equilibrium configuration possesses certain symmetry elements. These correspond to symmetry operations which interchange identical nuclei in the molecule. For example, the planar propynal molecule may be subjected to the symmetry operations σ_h, reflection in the molecular plane, and also

formally, E the identity operation. It is therefore classified under the C_s point group. This group has two irreducible representations, or "symmetry species" labelled A' and A". Neither of these representations are degenerate, and their character systems under the group operations are shown in Table 1. Translational and rotational displacement vectors for the molecule also generate representations of the C_s group, and their classifications are also given in Table 1. The x and y coordinates are taken to lie in the molecular plane and the z axis is perpendicular to this. Table 2 shows direct products for the C_s point group; these are obtained by multiplication of corresponding characters belonging to the two irreducible representations in Table 1, e.g. $\Gamma(A') \Gamma(A'') = \Gamma(A'')$.

When the 3N displacement coordinates for the atoms are written in the form of a column vector, application of the group symmetry operations generates a set of transformation matrices whose characters are readily determined. Thus we may apply this to the Cartesian displacement coordinates (x_i, y_i and z_i) attached to each atom, of which there are a total of 3N = 18 for propynal. The identity operation leaves all these displacements unchanged, and the corresponding matrix is unitary and of dimension 18, therefore the character $\chi(E) = 18$. Under the σ_h operation, the x and y displacement coordinates in the molecular plane remain unchanged, and constitute + 12 to $\chi(\sigma_h)$; but the z coordinates are changed in sign and contribute -6 to the character. So the representation generated is

TABLE 1

THE CHARACTER TABLE FOR THE C_s POINT GROUP

	E	σ_h		
A'	1	1	T_x, T_y	R_z
A"	1	-1	T_z	R_x, R_y

TABLE 2

THE DIRECT PRODUCTS TABLE FOR THE C_s POINT GROUP

	A'	A"
A'	A'	A"
A"	A"	A'

	E	σ_h
Γ_D	18	6

The characters of these matrices remain unchanged by the similarity transformation that transforms the Cartesian coordinates (x_i, y_i, z_i) into the 3N normal coordinates Q_i. Therefore decomposition of Γ_D into its irreducible representations yields the number and symmetries of the normal modes of motion of the molecule. However, we note that the 3N degrees of freedom defined by 3N coordinates include the three translational and three rotational motions of the molecule. Table 1 shows that these have the characters

	E	σ_h
$\Gamma_{(T)}$	3	1
$\Gamma_{(R)}$	3	-1
$\Gamma_{(T_1R)}$	6	0

When these are subtracted from Γ_D, there results the character system $\Gamma_v = (12,6)$ for the purely vibrational modes. This can be decomposed into its irreducible components with the aid of Table 1 to give

$$\Gamma_v = 9\,\Gamma_{(A')} + 3\,\Gamma_{(A'')} \qquad (2.12)$$

Therefore out of the twelve total normal modes of vibration of the molecule, nine are directed along normal coordinates lying in the molecular plane and belong to the A' representation, and three are directed out of the plane and belong to the A" representation.

III. SELECTION RULES FOR INFRA-RED TRANSITIONS: The probability of a transition between two vibrational states ψ'_v and ψ''_v in a molecule is proportional to the square of the vibrational transition moment R_v, where

$$R_v = \int \psi'_v \mu \psi''_v \, d\tau \qquad (2.13)$$

where μ is the dipole moment of the molecule with component μ_x, μ_y and μ_z along the Cartesian axis system attached to the molecule. R_v can be resolved into components

$$(R_v)_x = \int \psi'_v \mu_x \psi''_v \, d\tau \qquad (2.14)$$

$$(R_v)_y = \int \psi'_v \mu_y \psi''_v \, d\tau \qquad (2.15)$$

$$(R_v)_z = \int \psi'_v \mu_z \psi''_v \, d\tau \qquad (2.16)$$

and at least one of these components must differ from zero for a vibrational transition to be allowed. The selection rules can be readily determined by group theoretical methods, using the fact that the integrands in equations (2.14), (2.15) and (2.16) can only differ from zero if they belong to totally symmetric group representations. So the direct product $\Gamma(\psi'_v)\Gamma(\psi''_v)$ must belong to the same representation as at least one of the components μ_x, μ_y or μ_z for this to occur. The direct products for the two vibrational wavefunctions can be obtained from Table 2.

The components of the dipole moment are

$$\mu_x = \sum_i e_i x_i \quad \mu_y = \sum_i e_i y_i \quad \mu_z = \sum_i e_i z_i \qquad (2.17)$$

where e_i is the effective change on the ith atom. Since this remains

constant, the dipole moment components transform under the group operations in the same manner as the translational displacements T_x, T_y or T_z along the same spatial direction. Therefore, $\Gamma(\psi'_v)\Gamma(\psi''_v)$ must belong to the same representation A" as T_z for a transition polarised along the z axis to occur, and to the same representation A' as T_x and T_y for an in-plane transition to be allowed. It therefore follows that transitions in absorption from the vibrationless ground state A' symmetry to vibrational states of A" symmetry in propynal are out-of-plane polarised, and transitions to states of A' symmetry are in-plane polarised. In other words, the nine fundamental vibrations of A' symmetry yield infra-red bands that are in-plane polarised, whereas the three fundamental vibrations of A" symmetry give bands that are out-of-plane polarised.

CHAPTER 3

EXPERIMENTAL - THE INFRA-RED AND RAMAN SPECTRA

I. THE SYNTHESIS OF PROPYNAL: Propynal was prepared by the method of Willie and Saffer[4], the procedure following the method given in Organic Synthesis[5]. This consisted of the oxidation of 2-propyn-1-ol with chromic acid. To an agitated mixture of 360 mls. of the alcohol in 135 mls. of sulphuric acid and 200 mls. of water, was added dropwise a solution of 210 grms. of chromium trioxide, dissolved in 135 mls of sulphuric acid and 400 mls. of water. The reaction vessel was surrounded with a bath at 0°C and was maintained at a pressure of 15 mm Hg by evacuation with a water aspirator. A stream of nitrogen was bled into the reaction mixture and expelled the propynal before it could oxidise to the corresponding acid. The volatile products were passed through three traps in succession, the first being maintained at -10°C to remove water vapour, and the remaining two at dry ice temperature to collect the propynal.

The propynal and the water which still remained in the sample were separated into two phases by saturating the resulting product with an excess of potassium chloride. The organic phase was decanted, dried with anhydrous sodium sulphate and distilled through a 10" Podbielniak column with 60 theoretical plates. The centre fraction boiling between 54 - 56°C was collected. In subsequent preparations propynal was not distilled through the column but purified by

trap-to-trap distillation. This gave a product which had an infra-red spectrum identical in every way to the carefully purified compound.

The procedure of Costain and Morton[8] was used to prepare the d-acetylenic propynal DC≡CCHO. Dry purified propynal was added to 99.7% D_2O until a 50% mixture by volume was obtained. This was made alkaline by the dropwise addition of a dilute solution of sodium deuteroxide, until a brown polymeric material started to precipitate from the solution. At this pH, the exchange is known to be complete. The reaction vessel was quickly plunged into liquid nitrogen to prevent further polymerisation, then attached to a vacuum line and the volatile material distilled off and collected in a trap at liquid nitrogen temperature. The aqueous and organic components were separated into two phases, by salting out with KCl. The propynal was decanted, dried and purified by trap-to-trap distillation several times. The exchange procedure was repeated four times until the isotopic purity was estimated to be better than 95% deuterium. This was evaluated by comparing the absorbance of the bands at 2125 cm^{-1} and 2110 cm^{-1} in the infra-red spectrum which are ascribed to the (C≡C) mode ν_3 in HC≡CCHO and DC≡CCHO as shown in Chapter 4.

The d-aldehydic propynal HC≡CCDO was prepared by the Merck Chemical Company of Montreal, and was kindly donated to us by Dr. C. C. Costain of the National Research Council.

II. INFRA-RED SPECTRUM: A Perkin Elmer double beam spectrophotometer model 21 was used to record the infra-red spectrum. The regions from 4000 - 650 cm^{-1} and from 700 - 450 cm^{-1} were scanned with NaCl and KBr optics respectively. Slit widths varied from 15 microns at 4000 cm^{-1} to 10 microns at 600 cm^{-1}. Wave-length calibration of the spectrophotometer in the NaCl region was made using the spectra of water vapour and of polystyrene film. The uncertainty in measurement of the band origins is estimated to be $\pm$ 10 cm^{-1} at 4000 wavenumbers and $\pm$ 3 cm^{-1} at 600 cm^{-1}. The gas cell used to contain the propynal had a path length of 10 cm, and a diameter of 3 cm and was externally flanged to match the KBr windows. The flanges were ground flat, lightly coated with silicone grease and the windows placed into position at each end, being held there by maintenance of the cell at a pressure that was less than atmospheric. The vapour pressure of propynal within the cell, was adjusted by varying the temperature of the liquid substance contained in a bulb connected to the absorption cell. The bulb was immersed in slush baths at various temperatures, and it was possible to control the vapour pressure within the cell up to 164 mm. Hg. (the saturation vapour pressure at room temperature).

III. THE RAMAN SPECTRUM: The Raman spectrum of liquid propynal was obtained with a two-prism Hilger E615 Raman spectrograph. A vertically mounted spiral Toronto type, low pressure mercury arc was used for excitation. The striking potential was 250v DC and the operating current, 12 amps. Exposure times varying between 30

minutes and 3 hours were required when Kodak 103a-O and IIa-O plates were used. At room temperature, propynal slowly polymerises into a reddish-brown polymeric material, which completely absorbs the 4358 Å exciting line, a process which is markedly enhanced by the action of the exciting light. A jacketed Raman cell was constructed, (illustrated in Figure 1) that was designed to operate between -20° and 25°C. The inner cell (a) contained 15 ml. liquid propynal. This was surrounded by a jacket (b), through which coolant flowed. An annular space (c) was filled with dry nitrogen and provided insulation between the filter jacket (d), containing saturated sodium nitrite solution, and the cooling jacket (b). To prevent the formation of ice crystals on the cell window, a second window was attached, which was separated from the cold inner cell by an insulating air space (f).

The Raman plates were microphotometered with a Leeds and Northrup travelling microphotometer. To obtain the wavenumbers of the Raman lines a dispersion curve was constructed to the same scale as the microphotometer trace from suitable iron and Hg arc reference lines. The Raman lines in the microdensitometer record were calibrated by interpolation from the dispersion curve.

Depolarisation studies were made using the method suggested by Edsal and Wilson[6]. Polaroid cylinders (e) were slipped into the annular space (c) between the inner and outer jacket to polarise the light from the Hg arc parallel and perpendicular to the optic axis of the spectrograph. Exposures with parallel and perpendicular

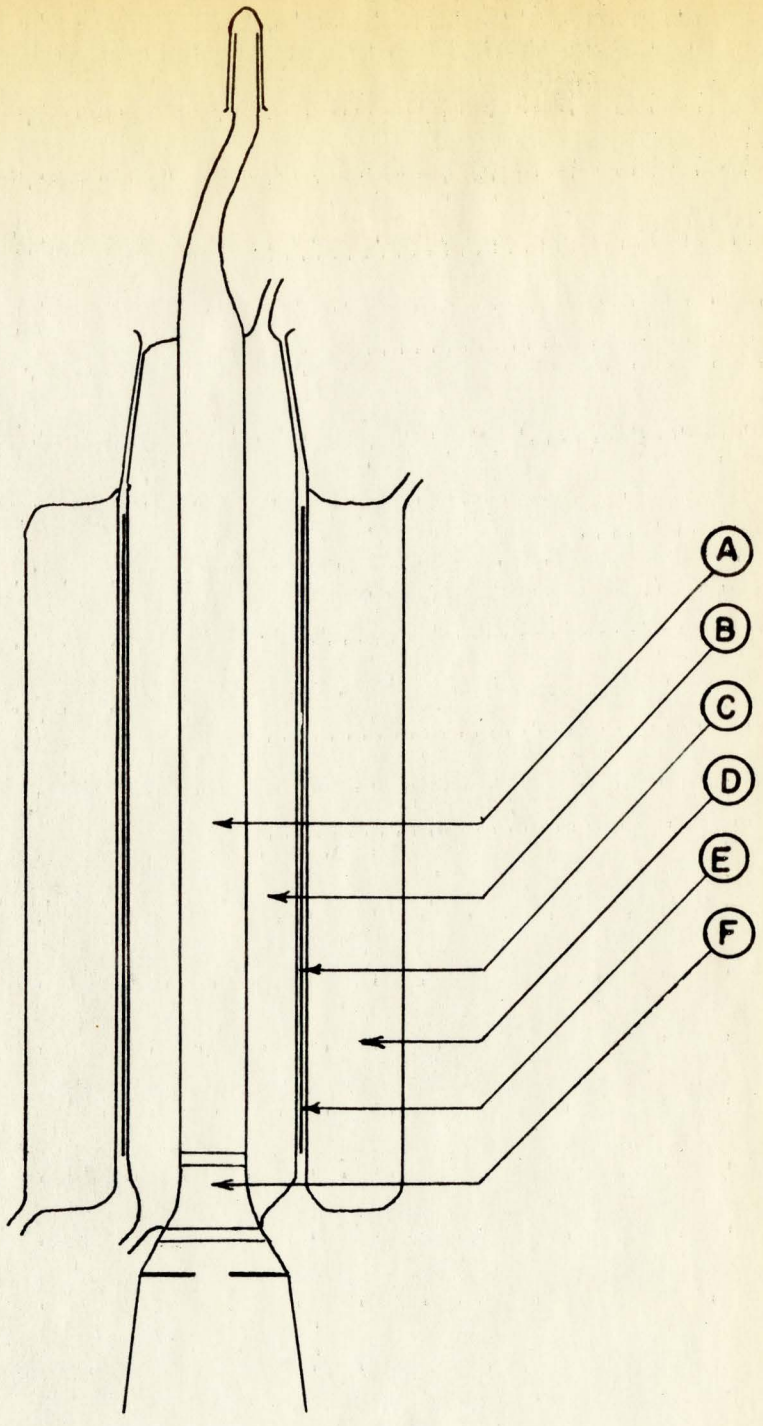

FIG. I THE RAMAN CELL

polarised light were taken on the same spectroscopic plate and the intensities of the Raman lines compared visually.

CHAPTER 4

THE ANALYSIS OF THE INFRA-RED AND RAMAN SPECTRUM

I. INTRODUCTION: The infra-red spectra of gaseous HC≡CCHO, HC≡CCDO and DC≡CCHO are shown in Figures 2 and 3, and the microdensitometer trace of the Raman spectrum of liquid HC≡CCHO in Figure 4. The wavenumbers of the centres of the infra-red bands and of the Raman lines are collected in Tables 3 and 4.

The infra-red spectrophotometer was unable to resolve the rotational structure of the bands, but two types of vibrational bands were apparent in the spectra, namely, those which exhibited well defined symmetrical doublets with maxima separated by 15 cm^{-1}, and those which extended over several hundred wavenumbers and possessed weak sub-structure with maxima separated by 10 cm^{-1}.

In the Raman spectrum each vibrational band appeared as a single peak projecting out of a continuous background. This background was weak at 4000 Å and reached maximum intensity at 6000 Å. In Chapter 7, it is shown that this continuum may be attributed to the emission spectrum of propynal which has an electronic origin at 4144 Å. In the Raman spectrum, the Hg exciting line at 4358 Å was surrounded by a region of continuous emission (presumably due to the unresolved rotational Raman spectrum) which extended over a range of several hundred wavenumbers. This made accurate measurements of the wavenumbers of the two Raman lines that occurred at displacements

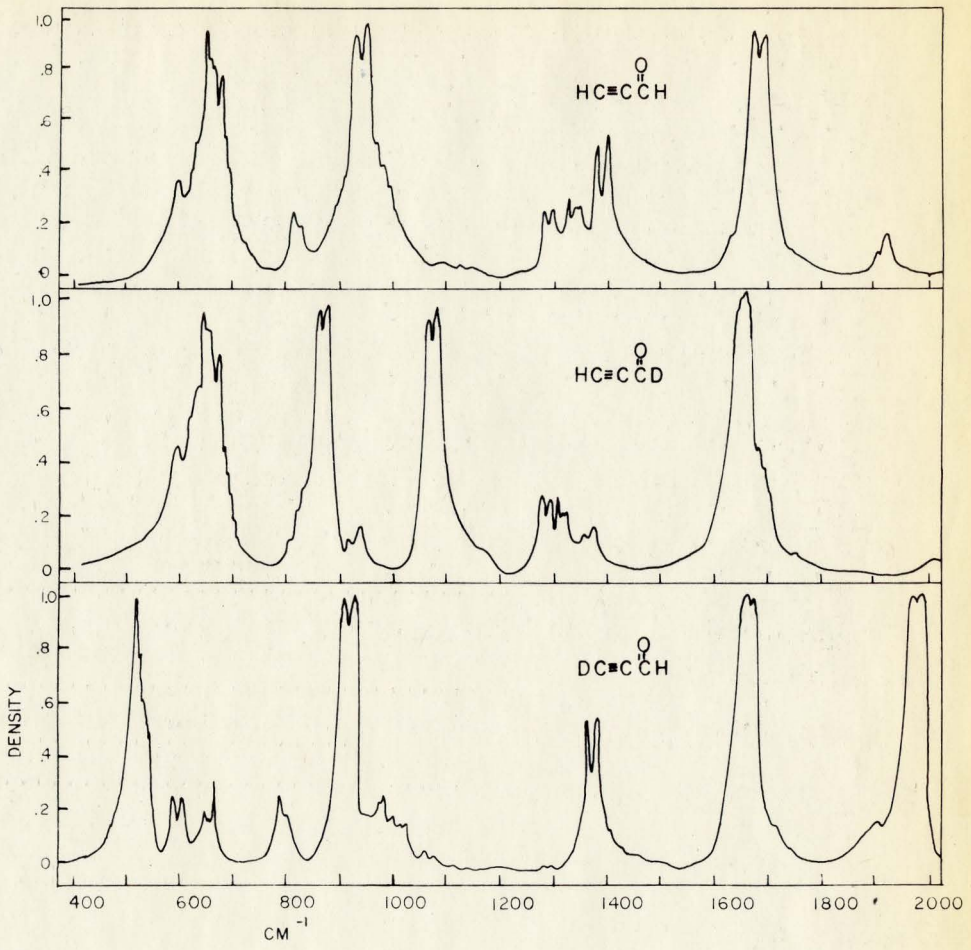

FIG. 2 INFRA-RED SPECTRA

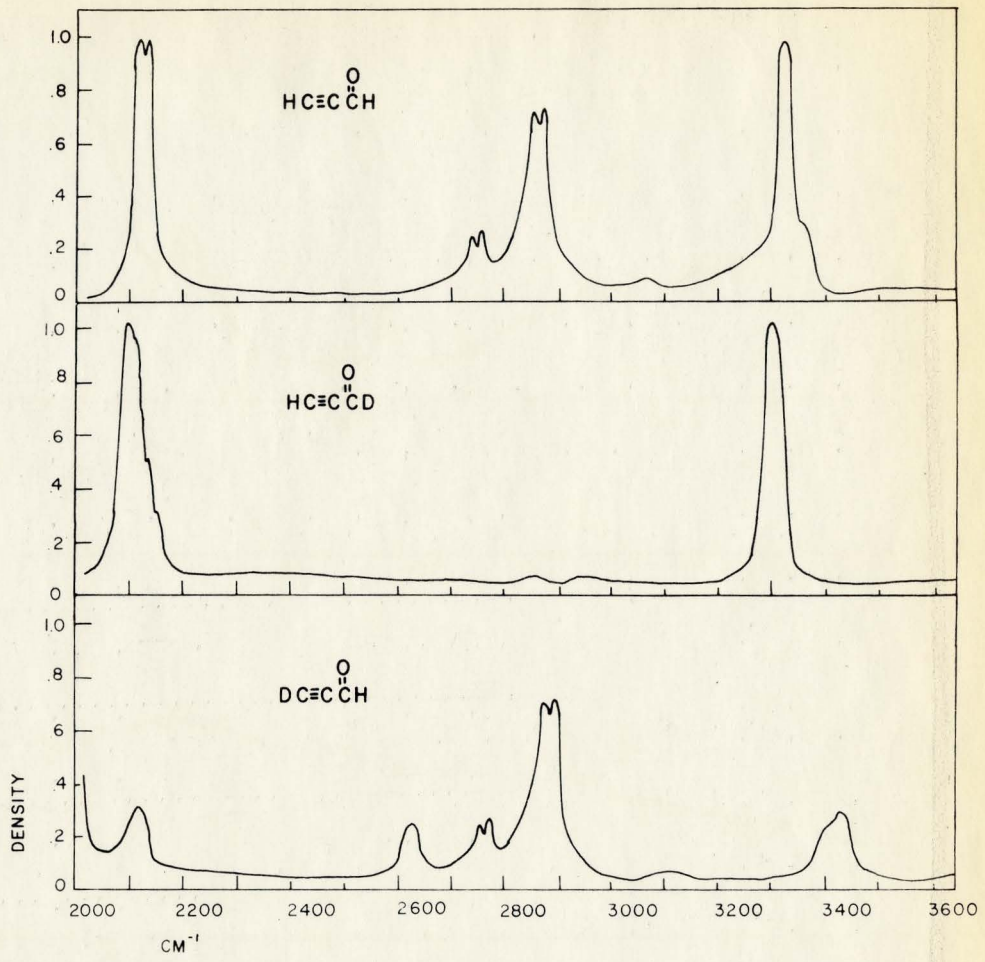

FIG. 3 INFRA-RED SPECTRA

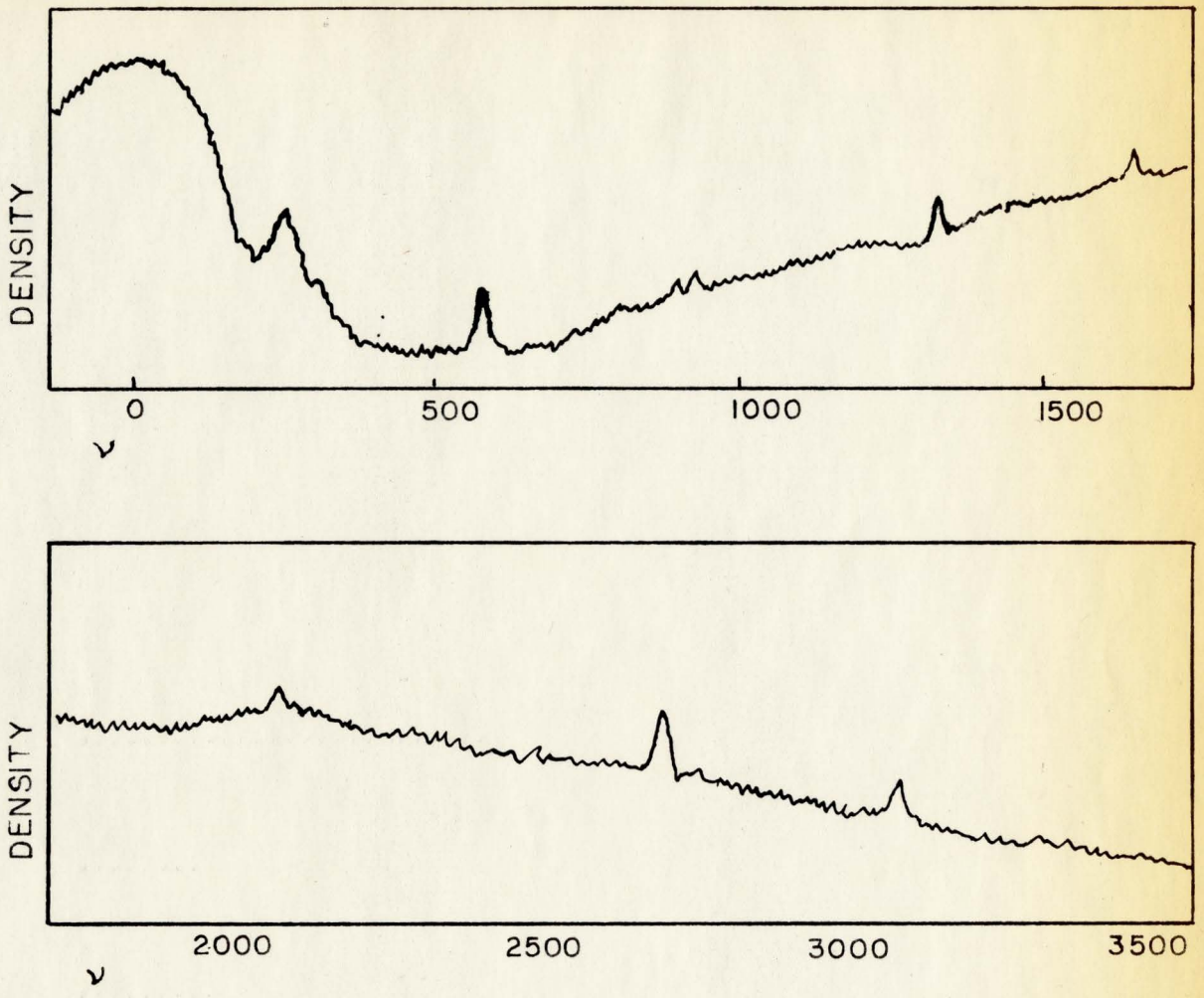

FIG. 4 THE RAMAN SPECTRUM
OF LIQUID HC≡CCHO

TABLE 3

WAVENUMBERS AND ASSIGNMENTS OF THE INFRA-RED BANDS OF PROPYNAL

HC≡CCHO		HC≡CCDO		DC≡CCHO		Assignment and symmetry
cm^{-1}	I	cm^{-1}	I	cm^{-1}	I	
3380	(m,sh)					
				3440	(m)	
3335	(vs)	3300	(vs)			$\nu_1(a')$
3080	(vw)			3100	(vw)	
2869	(s)	(2870)*	(vw)	2880	(s)	$\nu_2(a')$
2780	(m)			2780	(m)	$2 \times \nu_5(a')$
				2620	(m)	$\nu_1(a')$
		2300	(vw)	2132	(m)	
		2130	(m,sh)			$\nu_2(a')$
2125	(vs)	2110	(vs)	1990	(vs)	$\nu_3(a')$
1925	(w)			1900	(w)	$2 \times \nu_{10}(a')$
				1700	(w,sh)	
1692	(vs)	1670	(vs)	1682	(vs)	$\nu_4(a')$
1398	(ms)			1379	(ms)	$\nu_5(a')$
		1380	(w)			$2 \times \nu_{10}(a')$
1340	(m)	1320	(m)			$2 \times \nu_7(a')$
1275	(m)	1275	(m)			$2 \times \nu_{11}(a')$
		1076	(vs)			$\nu_5(a')$

$HC\equiv CCHO$		$HC\equiv CCDO$		$DC\equiv CCHO$		Assignment and symmetry
cm^{-1}	I	cm^{-1}	I	cm^{-1}	I	
990	(m,sh)			980	(m)	$\upsilon_{10}(a")$
950	(vs)	871	(vs)	923	(vs)	$\upsilon_{6}(a')$
815	(w)	871	(w,sh)	815	(w)	$\upsilon_{8} + \upsilon_{12}(a")$
691	(s,sh)	681	(s,sh)	(680)*	(w)	$\upsilon_{7}(a')$
669	(s)	659	(s)			$\upsilon_{11}(a")$
615	(w)	615	(w)	615	(w)	$\upsilon_{8}(a')$
				542	(w,sh)	$\upsilon_{7}(a')$
				519	(s)	$\upsilon_{11}(a")$

* Bands ascribed to impurities
s = strong, m = medium, w = weak, v = very,
sh = shoulder, p = polarised, dp = depolarised

TABLE 4

FREQUENCIES AND ASSIGNMENTS OF THE RAMAN LINES OF LIQUID PROPYNAL, HC CCHO

HC≡CCHO cm-1	I	Assignment and symmetry
3381	(w,p)	$\upsilon_1(a')$
2856	(w,p)	$\upsilon_2(a')$
2080	(m,p)	$\upsilon_3(a')$
1658	(s,p)	$\upsilon_4(a')$
1392	(s,p)	$\upsilon_5(a')$
988	(w,dp)	$\upsilon_{10}(a'')$
947	(vw,p)	$\upsilon_6(a')$
710	(vw,d)	$\upsilon_7(a')$ and $\upsilon_{11}(a'')$
620	(s,p)	$\upsilon_8(a')$
261	(m,p)	$\upsilon_9(a')$
226	(s,dp)	$\upsilon_{12}(a'')$

* Bands ascribed to impurities.

s = strong, m = medium, w = weak, v = very, sh = shoulder, p = polarised, dp = depolarised.

of 226 and 261 cm^{-1} from the exciting line difficult to obtain.

As has been shown in Chapter 2, of the 12 normal modes of vibration, 9 lie in the plane of the molecule and belong to the totally symmetric A' representation of the C_s point group, while the remaining 3 are directed out of the plane and belong to the A" representation.

Since the geometry of propynal is such that the molecule is almost a symmetric top in the ground electronic state, the vibrational bands in a first approximation can be classified in the same manner as symmetric top bands, i.e as perpendicular or parallel according to whether the transition moment is directed perpendicular or parallel to the symmetric top axis which has least moment of inertia. A rough calculation of the band contours, using the symmetric top approximation and the dimensions obtained for the ground state of propynal by microwave studies (with $\bar{B} = (B+C)/2$) showed that a parallel type band, in which an in-plane A' vibration is excited, should exhibit intense P and R branches whose maxima are separated by 15 cm^{-1} at room temperature, and that a perpendicular type band, in which an A" vibration is excited, should have an extended rotational structure with numerous weak K sub-bands on either side of the band origin. This enabled the polarisation of the observed bands to be determined.

The contours of the vibrational bands in the Raman spectrum of liquid propynal could not be used in similar manner as an aid to their assignment. However, depolarisation measurements on the Raman spectra enabled the bands to be assigned as in-plane or

out-of-plane vibrations according to whether they were polarised or depolarised respectively. The observed depolarisations are given in Table 4.

II. THE ASSIGNMENT OF THE FUNDAMENTAL BANDS IN THE INFRA-RED SPECTRUM:

The vibrational assignments for the ground electronic state were based on the evidence provided by the contours of the infra-red bands, the depolarisation of the Raman lines and the change in frequency of the vibrational modes on isotopic substitution. The ground state fundamental frequencies of propynal and their assignment are summarised in Table 5.

CH stretching vibrations are known to fall in the 2700 - 3400 cm^{-1} region and, as a result, the assignment of the vibrational modes ν_1 and ν_2 was quite straightforward for propynal. Since the intense band which appeared at 3335 cm^{-1} in the spectrum of normal propynal was shifted to 3300 cm^{-1} in d-aldehydic propynal and dropped to 2620 cm^{-1} in d-acetylenic propynal, it was assigned to the in-plane valence vibration ν_1. The reason for the weakness of the 2620 cm^{-1} band in DC≡CCHO was not obvious. As expected, there was little difference between the wavenumbers of ν_2, the aldehydic hydrogen stretching mode in HC≡CCHO and DC≡CCHO which are at 2869 and 2880 cm^{-1} respectively, whereas in HC≡CCDO, the wavenumber decreases to ~2130 cm^{-1}.

The wavenumbers of the (C≡C) and (C=O) modes ν_3 and ν_4 are not expected to display large shifts on deuteration. The ν_3 vibration is located mainly in the (C≡C) group but also involves

TABLE 5

SUMMARY OF THE GROUND STATE FUNDAMENTAL FREQUENCIES (CM^{-1}) OF PROPYNAL

Infra-red (vapour)			Raman (liq.)	
HC≡CCHO	HC≡CCDO	DC≡CCHO	HC≡CCHO	Assignment
3335	3300	2620	3381	ν_1 acet. CH stretch
2869	2130	2880	2856	ν_2 ald. CH stretch
2125	2110	1990	2080	υ_3 C≡C stretch
1692	1670	1682	1658	ν_4 C=O stretch
1398	1076	1379	1392	ν_5 HCO bend
950	871	923	947	ν_6 C-C stretch
691	681	542	(710*)	ν_7 HC≡C bend
615	615	615	620	υ_8 CCO bend
			261	ν_9 CCC bend
990	650	980	988	ν_{10} HCO bend
669	659	519	710*	ν_{11} HC≡C bend
			226	ν_{12} CCC bend

* Very diffuse

small motions of the acetylenic hydrogen. The frequency of ν_3 should therefore decrease slightly upon acetylenic, but not aldehydic deuteration. Conversely, the frequency of the (C=O) ν_4 mode should be insensitive to acetylenic deuteration and decrease slightly on aldehydic deuteration. The frequency of the bands assigned to these modes in Table 5 behave in the manner predicted.

The in-plane bending motion of the aldehydic hydrogen atom has a frequency of 1378 cm^{-1} in formamide[7] and 1371 cm^{-1} in methyl formate[8]. The intense bands at 1398 cm^{-1} and 1379 cm^{-1} in HC≡CCHO and DC≡CCHO were therefore assigned to the corresponding ν_5 mode in propynal. The band at 1076 cm^{-1} in HC≡CCDO is assigned to this mode. The apparently high intensity of this band is due to another underlying band of which traces can be seen.

The ν_6 vibration, essentially a C-C stretching mode, was assigned to bands at 950 cm^{-1} and 923 cm^{-1} in HC≡CCHO and DC≡CCHO respectively. There are two strong bands in HC≡CCDO at 1076 cm^{-1} and 871 cm^{-1} and since the higher of these was ascribed to the (CDO) mode ν_5, the 871 cm^{-1} band was assigned to ν_6. The separation of these two bands may be increased by a Fermi resonance.

In the 500 - 700 cm^{-1} region, each spectrum shows a strong band of complex structure that is almost identical in HC≡CCHO and HC≡CCDO, but is shifted to lower frequency and altered in DC≡CCHO. In each case, the prominent features are a single intense peak belonging to a perpendicular type band, with a hybrid type band, showing P and R wings separated by 15 cm^{-1}, on

its high frequency shoulder. The pair of bands were assigned to the υ_{11} out-of-plane and υ_7 in-plane acetylenic hydrogen bending motions, which are expected to differ slightly in frequency. Nyquist and Potts[9], have recently given arguments, applicable to propynal, for assigning the lower frequency to the out-of-plane vibration in such terminal acetylenic groups.

The υ_{10} vibration appeared clearly only in DC≡CCHO as a single peak at 980 cm^{-1} with adjacent structure conforming to that predicted for a perpendicular type band. The same vibration is at 1030 cm^{-1} in formamide and 1032 cm^{-1} in methyl formate. In HC≡CCHO the band appeared on the high frequency shoulder of the strong υ_6 band; in HC≡CCDO it was buried beneath the complex at 650 cm^{-1}.

III. THE ASSIGNMENT OF THE COMBINATION BANDS IN THE INFRA-RED SPECTRUM:

Because of the low symmetry of propynal, a large number of combination bands are possible and Fermi resonances can readily occur. It was pointless to attempt assignments of all observed weak bands in Table 3, but some tentative correlations were made of certain features that resemble each other in shape and intensity in the infra-red spectra of the three isotopic species.

Identical parallel type bands at 2780 cm^{-1} appear in HC≡CCHO and DC≡CCHO; if these are $2\times\upsilon_5$ the corresponding band in HC≡CCDO will be beneath that at 2110 cm^{-1} and hence be unobserved. Bands identifiable as $2\times\upsilon_{10}$ are visible in all three spectra. If the $2\times\upsilon_7$ and $2\times\upsilon_{11}$ features were correctly identified in HC≡CCHO and HC≡CCDO, then they will be hidden beneath the absorption in the 900 - 100 cm^{-1}

region in DC≡CCHO. HC≡CCHO and DC≡CCHO show similar perpendicular type bands at 815 cm^{-1} ascribed to ν_8 and ν_{12}; these low frequency bands cannot involve hydrogenic vibrations combined with other vibrations, and so the analogous band in HC≡CCDO would be at similar frequency but submerged beneath a stronger absorption.

Lastly, there is a distinct weak band in DC≡CCHO at 3440 cm-1. This could not be identified but may well involve motion of the acetylenic deuterium atom, its counterpart in HC≡CCHO and HC≡CCDO being shifted to higher frequencies beyond the region of observation.

IV. THE ANALYSIS OF THE RAMAN SPECTRUM: The vibrational assignment of the lines in the Raman spectrum of liquid HC≡CCHO confirm the analysis of the infra-red spectrum of gaseous propynal. The relative intensities of the bands in the Raman spectrum differ from the intensities of the corresponding infra-red bands. As a result of a strong intermolecular association between propynal molecules in the liquid, the frequencies of the corresponding bands in the infra-red and Raman spectrum are not expected to be the same. A strong hydrogen bond between the non-bonding electrons of the p orbital of the oxygen atom and the acetylenic hydrogen atom, (C-H...O = C), should reduce the frequency of the (C-H) and (C=O) stretching modes ν_1 and ν_4 and increase the frequency of the (C≡CH) and (C-C=O) bending modes ν_7, ν_8 and ν_{11}. The difference in wavenumbers between the infra-red and Raman bands corresponding to ν_4, ν_8 and ν_{11} are in the direction predicted. However, ν_1 is anomalous in

that the frequency is lower in the vapour than in the liquid state. The frequencies of the vibrational modes υ_2, υ_5 and υ_{10}, which involve motions of the aldehydic hydrogen atom are not shifted appreciably between the vapour and liquid states, which indicates that the aldehydic hydrogen atom is very weakly associated in the liquid phase.

The two diffuse bands located at 226 cm^{-1} and 261 cm^{-1} were assigned to the remaining skeletal modes υ_9 and υ_{12}. Howe and Goldstein[1] obtained rough values of 150 $\pm$ 15 cm^{-1} and 230 $\pm$ 10 cm^{-1} for these modes from the intensity alteration of the microwave spectrum with changing temperature. A visual comparison of the Raman spectra recorded on the same spectral plate, excited by light from the Hg arc, polarised parallel and perpendicular to the axis of the spectrograph, indicated that the 261 cm^{-1} Raman line was polarised and the 226 cm^{-1} line depolarised, although interference by the underlying continuous emission made this assignment somewhat uncertain. On this basis, the υ_9 mode was assigned to the 261 cm^{-1} band and the 226 cm^{-1} band assigned to the υ_{12} mode. In order to analyse the vibrational structure in the band spectrum, it was necessary to reverse the assignment of these two low frequency modes as shown in Chapter 7.

CHAPTER 5

THEORY OF ULTRAVIOLET SPECTRA

I. ELECTRONIC TRANSITIONS: We use here the simple LCAO/MO description for the electronic states of propynal. The optical electrons, which can be excited in spectroscopic transitions of low energy, occupy two main types of molecular orbital - 1) π - type orbitals which extend over several atomic centres in the molecule, and which are subdivided into π or π^* orbitals according to their relative bonding or antibonding properties; 2) n - type orbitals which are primarily localised on one atomic centre, which is the oxygen atom in the case of propynal.

To a first approximation, we may consider the near-ultraviolet absorption spectrum of propynal as arising from the excitation of electrons localised in the carbonyl group. Absorption in this spectral region with relatively weak intensity is characteristic of the $n \longrightarrow \pi^*$ transition that carbonyl-containing compounds exhibit. On the other hand, the $\pi \longrightarrow \pi^*$ transitions that are characteristic of compounds containing acetylenic groups lie usually in the 2000-2500 Å region.

Our discussion below of the intensity and polarisation of the singlet-triplet spectrum of propynal is, therefore, primarily in terms of the local symmetry of the carbonyl group, following Platt's notation[11]. Following Nason[12], we schematically represent the ordering

of the energies of the local molecular orbitals as in Figure 5. The lowest energy σ orbital and its anti-bonding counterpart σ^* are directed along the C=O bond. The π and π^* orbitals are formed by the in-phase and out-of-phase overlap of the p_z atomic orbitals that are centered on the carbon and oxygen atoms and project above and below the molecular plane. The non-bonding n orbital is the 2p orbital on the oxygen atom that is in the molecular plane and perpendicular to the C=O bond.

The intensity of an optical transition between two electronic states of a molecule is dependent upon the transition moment, equation (1.7). We assume that a transition can be represented by the promotion of a single electron from one molecular orbital to another, and write the transition moment for an $n \longrightarrow \pi^*$ transition as

$$R = \int n(i)\, \mu(i)\, \pi^*(i)\, d\tau \qquad (5.1)$$

where n(i) and $\pi^*(i)$ are the single electron wavefunctions for the promoted ith electron. The promotion of a single electron from the n orbital in the ground state to the π^* orbital in the excited state is illustrated in Figure 5. The intensity of a transition at wavenumber ν is usually described in terms of the oscillator strength f, which is related to the transition moment by

$$f = (1.085 \times 10^{-5})\, \nu\, R^2 \qquad (5.2)$$

This quantity is determined experimentally by integration of the molecular extinction coefficient

$$f = (4.39 \times 10^{-9}) \int \varepsilon\, d\nu \qquad (5.3)$$

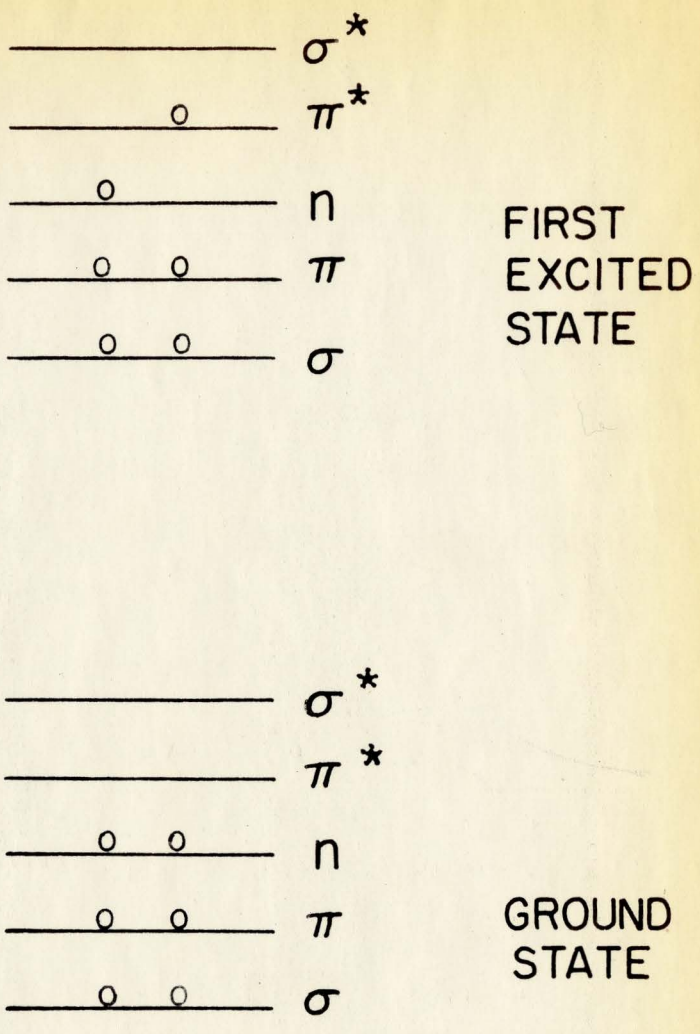

FIG.5 THE $n \rightarrow \pi^*$ TRANSITION IN THE CARBONYL CHROMOPHORE

In the single electron approximation of equation (5.1), the integrand at each point in configuration space is small if there is little overlap between the n and π^* orbitals. The transition probability R is, therefore, small when the n orbital is the pure p orbital on the oxygen atom, and is orthogonal to the out-of-plane p_z orbitals on the carbon and oyxgen atoms which combine to form the π^* molecular orbital. These $n_o \longrightarrow \pi^*$ transitions are very weak in carbonyl-containing compounds, with oscillator strengths of $f \sim 10^{-4}$; they are, in effect, forbidden by the local symmetry of the carbonyl group orbitals and are called $^1u \leftarrow {}^1A$ in Platt's notation. The lowest singlet-singlet transition in propynal is undoubtedly of this type.

II. SELECTION RULES FOR ELECTRONIC TRANSITIONS: The symmetry of the vibronic wavefunction $\psi_e\psi_v$ for a molecule is given by the direct product $\Gamma(\psi_e)\Gamma(\psi_v)$ of the representations of the molecular point group to which ψ_e and ψ_v belong. The transition moment integral

$$\psi'_{ev} u \psi''_{ev} d\tau \qquad (5.4)$$

for electric dipole-allowed transitions between different vibronic states must transform like, or have a component which transforms like the totally symmetrical representation of the point group, which is the A' representation for the C_s point group to which propynal belongs under the group symmetry operations. This means that the direct product $\Gamma(\psi'_{ev})\Gamma(\psi''_{ev})$ must transform like the dipole moment operator u, or, more generally, like one of its Cartesian

components. These transform like translations along the corresponding axes. As shown in Figure 6, the z axis is perpendicular to the molecular plane, and the x and y axes are any two axes at right angles to each other in the molecular plane. Therefore, according to Tables 1 and 2

$\Gamma(\psi'_{ev})\Gamma(\psi''_{ev})$ must transform like the A' representation for a transition polarised in the molecular plane

$\Gamma(\psi'_{ev})\Gamma(\psi''_{ev})$ must transform like the A" representation for a transition polarised perpendicular to the molecule plane.

When no vibrations are excited in an electronic state, ψ_v is totally symmetric. The ground electronic state of propynal also belongs to the totally symmetric A' representation. So ψ''_{ev} is totally symmetric and the (0-0) band for the electronic transition to an A' electronically excited state will be in-plane polarised, whereas if the excited state is A", it will be out-of-plane polarised. For example, the lowest singlet excited state of propynal has A" electronic symmetry, and the (0-0) band does indeed resemble a perpendicular-type band for the symmetric top to which propynal closely approximates, and the transitions from the ground vibronic states to the excited electronic state, where in-plane (A') vibrations are excited also have perpendicular-type contours. We show below how the contours are different for corresponding bands in the singlet-triplet transition.

So far, we have only determined the direction of the transition moments. In the absence of spin-orbit interaction terms in the

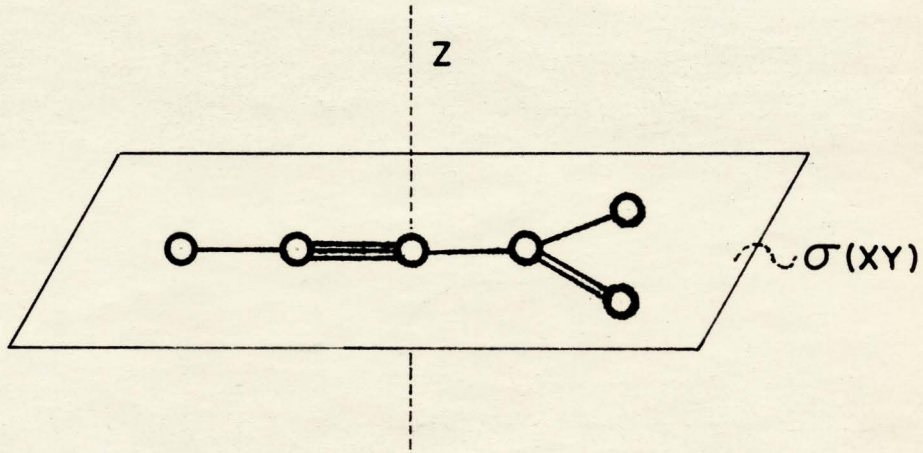

FIG. 6 THE SYMMETRY ELEMENTS OF PROPYNAL

Hamiltonian operator for the molecule, the singlet-triplet transitions have zero intensity. When these interaction terms are included, the zeroth-order wavefunctions $(\psi_e \psi_s)^\circ$ can mix with each other if they have the same symmetry, i.e. the wavefunction for each state, becomes a linear combination of all states with the same symmetry for the complete electronic wavefunctions.

If $(\psi_e^T \psi_s^T)^1$ represents the first order wavefunction for the lowest triplet state when singlet states $(\psi_e^S \psi_s^S)_i^\circ$ of the same symmetry are mix with it, then the expansion, apart from normalisation factors, has the form

$$(\psi_e^T \psi_s^T)^1 = (\psi_e^T \psi_s^T)^\circ + \sum_i c_i (\psi_e^S \psi_s^S)_i^\circ \qquad (5.5)$$

The intensity of the transition between the unperturbed ground state $(\psi_e^S \psi_s^S)_o^\circ$ and the triplet state is governed by the transition moment integral

$$\int (\psi_e^T \psi_s^T)^1 |\mu| (\psi_e^S \psi_s^S)_o^\circ \, d\tau \qquad (5.6)$$

which on substituting from equation (5.5) gives

$$\int \sum_i c_i (\psi_e^S \psi_s^S)_i^\circ |\mu| (\psi_e^S \psi_s^S)_o^\circ \, d\tau \qquad (5.7)$$

since

$$\int (\psi_e^T \psi_s^T)^\circ |\mu| (\psi_e^S \psi_s^S)_o^\circ \, d\tau = 0 \qquad (5.8)$$

Equation (5.7) shows that the polarisation of the triplet-singlet transition is the same as that of the singlet-singlet transition between states of the same total symmetry. The components of the triplet state, with symmetries A' and A", can mix with singlet states of the same symmetry and the triplet-singlet transition thus acquires finite intensity.

III. SINGLET-TRIPLET TRANSITIONS: We now introduce a wavefunction ψ_s for the total electron spin of the molecule, so that the vibronic wavefunction becomes $\psi_e \psi_v \psi_s$. We shall, however, ignore the vibrational wavefunction ψ_v in the discussion below, and call $\psi_e \psi_s$ the complete electronic wavefunction. Once the symmetry properties of this function, and the electronic polarisation of the singlet-triplet transition, have been determined, we can then determine the polarisations of transitions between vibronic states in the manner described in the previous section.

The spin function ψ_s for a singlet electronic state belongs to the totally symmetrical representation of the molecule point group,[13] and, therefore, has A' symmetry for propynal. The three spin functions ψ_s for the components of a triplet state belong to one dimensional rotational representations ; in other words, they belong to the same representations as the rotations R_x, R_y and R_z, so that for propynal two spin functions have A", and one spin function has A' symmetry.

In the singlet ground state, both ψ_e and ψ_s, belong to the A' representation. In the lowest triplet state, ψ_e has A" symmetry, which when combined with the symmetries of the spin functions ψ_s, shows that the symmetry of the complete wavefunction $\psi_e \psi_s$ is A' for two components and A" for one component.

Since in an electric dipole transition, the integrand over the complete wavefunction for the two combining states must be totally symmetrical, we find that for the transition between the

ground state and the lowest triplet state,

> the transition to two components of the triplet state ($A' \leftarrow A'$) is polarised in the molecular plane
>
> the transition to one component of the triplet state ($A'' \leftarrow A'$) is polarised perpendicular to the molecular plane.

We now investigate in greater detail which singlet states can mix with the components of the lowest triplet state with the same symmetry. The spin-orbit interaction operators H' mixes, in zeroth order approximation, triplet and singlet electronic states ψ_e^T and ψ_e^S with matrix elements.

$$\int \psi_e^T \, |H'| \, \psi_E^S \, d\tau \qquad (5.9)$$

Since the H' can only interchange spin functions among themselves, we can leave these functions out of the above integral in order to discuss the electronic symmetry

Since the Cartesian components H_x', H_y' and H_z' of H' transform under the group symmetry, operations like the corresponding rotations and the integrand in (5.5) must be totally symmetric, we have the possibilities,

$$\int \psi_e^T(A'') \, | \, H_x', \, H_y' | \, \psi_e^S(A') \, d\tau \qquad (5.10)$$

$$\int \psi_e^T(A'') \, | \, H_z' | \, \psi_e^S \, (A'') \, d\tau \qquad (5.11)$$

i.e. the spin operators H_x' and H_y' enable the $^3A''$ triplet state to mix with $^1A'$ singlet states, and H_z' mixes $^3A''$ with $^1A''$ states.

The singlet and triplet wavefunctions in (5.5) can each be expanded, in LCAO/MO approximation, as sums of one-electron orbitals. This problem of evaluating the corresponding matrix elements has been considered in detail by Sidman[14], for the case of mixing between low excited singlet states and the lowest triplet state of formaldehyde. Sidman makes the reasonable assumption that only one-centre integrals that do not vanish for symmetry reasons in the expansion have large magnitude; these integrals must be built from 2p atomic orbitals of different symmetry in the formaldehyde molecule. He assumes that the triplet state is perturbed by one singlet state and calculates the oscillator strength of the transition to be greatest when this state has the configuration in which one of the electrons in the π orbital in the ground state is promoted into the π^* orbital. A similar A' excited state of fairly low energy ($\sim$ 6-8eV) should exist for propynal, and Sidman's arguments can be similarly applied when only the local symmetry of the carbonyl group in propynal is considered. The mixing between $^3A''$ and this excited $^1A'$ state is enabled by the in-plane components of the spin-orbit interaction operator, equation (5.6).

The same conclusions may be reached from the generalised symmetry arguments of Krishna and Goodman[13]. The expansion of the matrix elements (5.5) into integrals over one-electron orbitals gives terms of the type

$$\int \pi |H'| \pi \, d\tau \qquad \int \pi |H'| n d\tau \qquad (5.12)$$

where π stands for either a π bonding or π^* anti-bonding orbital. The effect of operating upon an orbital with one of the components of H', say, H'_z , is equivalent to that of a rotation of the orbital around the z axis plus some other operation which produces no further change of symmetry. If the σ electron framework is ignored, and the reasonable assumption made that only the outer valence electrons in propynal contribute to the spin-orbit interaction, we see that only a rotation of the n orbital about an axis in the molecular plane can, in general, induce overlap with the π orbitals. Consequently, we expect that the components H'_x and H'_y will induce mixing, and therefore the perturbing singlet state has A' symmetry.

Now the perturbing state can only mix with these components of the triplet state which have the same A' symmetry for $\psi_e^T \psi_s^T$; it has been seen above that two of the three components have this symmetry and the transition to them from the singlet ground state is polarised in the molecular plane. This is seen later to agree with the experimental observations.

CHAPTER 6

EXPERIMENTAL - THE ULTRA-VIOLET SPECTRA

I. ABSORPTION SPECTRA, LOW RESOLUTION: A preliminary survey of the electronic spectrum of propynal, from 2000 to 7000 Å was made on a Perkin-Elmer Spectracord model 1000. The ultra-violet region 6500 - 2500 Å was also mapped with a Bausch and Lomb 1.5 meter grating spectrograph model 11. For the band spectra between 3900 Å and 3100 Å, it was found that path lengths of 50 cm. were sufficient to build up suitable absorption intensity, when the gas pressures varied between 10 mm. and 16 mm. Hg.

Since the absorption spectrum of propynal is extremely weak in the 4100 Å region, long path lengths and high vapour pressures of the absorbing gas were required. In order to obtain long absorption path lengths of gas, a multiple reflection cell was employed. In the multiple pass technique used[15] in this cell, as illustrated in Figure 7, light entered the absorption cell and was reflected back and forth a number of times between mirrors, mounted at either end, before passing into the spectrograph. Essentially, the optical arrangement within the cell consisted of three concave mirrors, two of which were positioned at the rear of the cell, in the same plane, while the remaining mirror was mounted at the front of the cell at the radius of curvature of the rear mirrors. Light passed through a notch (a) cut in one corner of the front

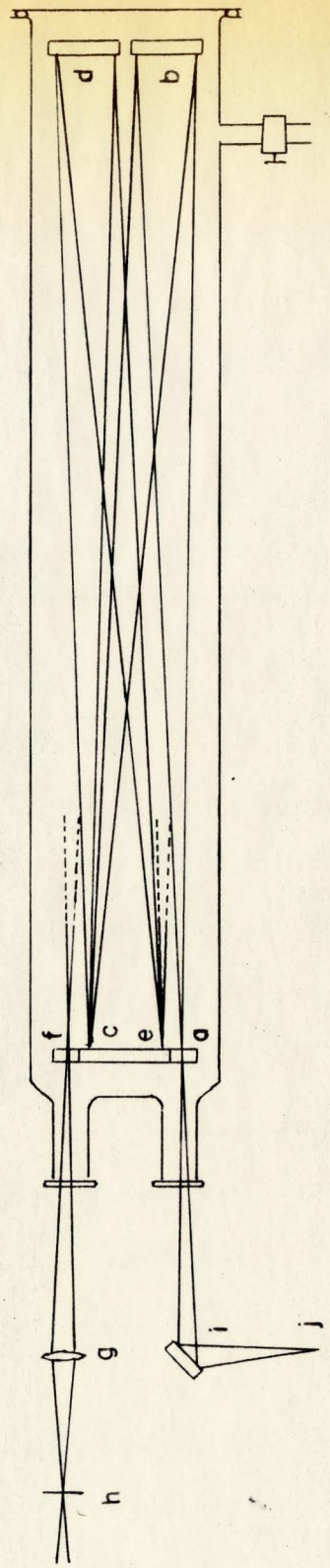

FIG.7 THE MULTIPLE REFLECTION CELL

mirror to rear mirror (b), where it was reflected back to point (c), on the front mirror. From here, the light was directed back to the other rear mirror (d) where it was reflected back to a point (e) on the front mirror and so on. In this way, the light was made to traverse the length of the absorption cell a maximum of 38 times before emerging through a second notch in the front mirror (f). By a suitable adjustment of the two rear mirrors (b) and (d) the path length could be varied between 60 meters and 4 meters. The multiple reflection mirrors, radius of curvature 1.85 meters, were mounted on brass supports by spring-loaded set screws, which allowed them to be rotated and positioned in all directions. The cell was constructed from a glass tube 10 cm. in diameter and 2 meters long. Entrance and exit windows were fixed to the front of the reflection cell and required frequent cleaning as a result of the formation of polymerised propynal on their surfaces. For this reason, it was also necessary to re-aluminise the mirror surfaces periodically.

The aperture of the Bausch and Lomb spectrograph was matched to the aperture of the multiple reflection cell by a fused silica lens of 40 cm. focal length (g). In order to align the external optics, a 6 volt car head lamp bulb was placed in the focal plane of the spectrograph in the plateholder aperture, and adjusted until a cone of green light was observed to pass out through the slit (h). Since this cone defined the optical aperture of the spectrograph it was traced through the focussing lens (g) into the multiple reflection cell where each traversal was aligned by adjusting the

mirrors. After emerging from the cell, the light was focussed by concave mirror (i) on the high pressure Xenon arc (j) used to generate the absorption continuum.

Attached to the multiple reflection cell was a glass vacuum line from which propynal was introduced into the system at known pressures. The propynal was purified by several trap-to-trap distillations before each experiment, in order to reduce the polymerisation within the cell during exposures.

The Bausch and Lomb grating spectrograph had a plate dispersion of 14.8 Å/mm and 7.4 Å/mm. in the first and second orders respectively with corresponding actual resolving power, $\nu/\Delta\nu$, of 35,000 and 70,000. The spectrograph was designed to cover the region 7400 - 3700 Å on a ten inch length of 35 mm. film, in the first order, or 3700 - 1830 Å in the second order. The overlapping orders were separated by inserting a 2 mm. thickness of Chance Bros. glass filters, either type OY10 or type OX 7, in front of the spectrograph slit. These filters transmitted the regions 3600 - 25,000 Å and 2400 - 4100 Å respectively.

The following 35 mm. photographic films were used in the low resolution studies - Ilford FP3, HPS and Kodak Spectrum Analysis #1 and #2. With the slit widths set at 10 microns, exposure times varied from 5 seconds to 30 minutes depending upon the number of traversals used in the multiple reflection cell and the speed of the photographic film. Iron arc reference spectra were also recorded on each film adjacent to the absorption spectra.

Development was carried out for 4 minutes in Kodak I.D.19 developer, in complete darkness, at a temperature between 17-20°C. After rinsing in plain water, the films were fixed for 10 minutes and then washed and dried in a dust free place.

The film was mounted between thin sheets of flat glass for support and the prominent features of the absorption spectrum, together with suitable iron arc lines were measured using a travelling microscope reading to 0.001 mm. The iron arc lines enabled a dispersion curve to be constructed from which the wave-lengths of the absorption bands were obtained by interpolation. These wave-lengths were converted into vacuum wave-lengths using Edlen's tables[16].

Microdensitometer records of the spectra were made with a Leeds and Northrup microphotometer. The film was scanned at a rate of 0.1mm/min. in most runs.

II. ABSORPTION SPECTRUM, HIGH RESOLUTION: High resolution spectra were taken in the first order of a 20 ft. Ebert grating spectrograph[17]. The plate dispersion was 0.66 Å/mm. in the first order and the theoretical resolving power of the spectrograph was 150,000. In the 30,000 cm^{-1} region, therefore, it should have been possible to resolve the lines with a separation of 30,000/150,000 = 0.2 cm^{-1}. In practice, lines separated by a 0.22 cm^{-1} were resolved, so that the actual resolving power was $\sim$140,000. Attempts to obtain better resolution by working in the second order failed, because this

necessitated using the grating almost at grazing incidence, and the intensity of the image is very low under these conditions.

The multiple reflection cell was aligned in front of the slit of the Ebert Spectrograph by the method described earlier. In order to remove stray light, and to ensure that the grating was evenly illuminated, a telescope was inserted into the plateholder aperture and focussed on to the grating image reflected by the spectrograph mirror. The external optics were then adjusted until the grating image was uniformly filled with light. Stray light was minimised by inserting stops in the external light beam.

Propynal was introduced into the absorption cell at known specific pressures from an auxiliary vacuum line. In order to eliminate pressure broadening, the total pressure within the absorption cell was maintained at less than 0.5 mm Hg. Only the more intense bands could be observed at these pressures. To photograph the weaker vibrational bands, vapour pressures up to 189 mm Hg. were required. At these pressures, the rotational structure of the vibrational bands was obliterated. Very weak bands were indistinguishable from the background absorption.

Observed sharp rotational structure in the (0-0) band was measured off the plate with a travelling microscope. Wave-lengths of the iron arc calibration lines were taken from the MIT tables[18], and were used to construct the dispersion curve, that is, the relationship between wave-length in air and position on the spectral plate. The theoretical plate dispersion was calculated from the

geometry of the spectrograph by the method of Callomon[15]. The resulting dispersion curve was described by a quadratic equation relating wavenumber and displacement across the spectral plates. All the rotational structure was not clearly resolved, and it was impossible to locate accurately the maxima of unresolved peaks in the spectrum with the travelling microscope. Consequently, the wavenumbers of these features were obtained by interpolation on microphotometer traces of the band, using as reference points the lines whose wave numbers were obtained directly from measurements off the plate.

III. THE EMISSION SPECTRUM: The emission spectrum of propynal was first observed when the Raman spectrum of the liquid was excited with the mercury line at 4358 Å, as a continuum between 4000 and 5500 Å on which the Raman lines were superimposed. This continuum was not due to scattering of the background radiation of the Hg lamp since it had a different intensity distribution.

The emission spectrum of the vapour was obtained using apparatus shown schematically in Figure 8. Propynal was introduced into the system at trap (a) and stored there at - 78°C until required. Immediately before each exposure it was purified by a trap-to-trap distillation between traps (a) and (b) and then stored in trap (c) maintained at 0°C during the experiment. Propynal vapour was passed through the capillary stopcock (d) which regulated the pressure in the emission cell (e). This cell was 1 cm. in diameter and 10 cm. long, and had a fused silica window

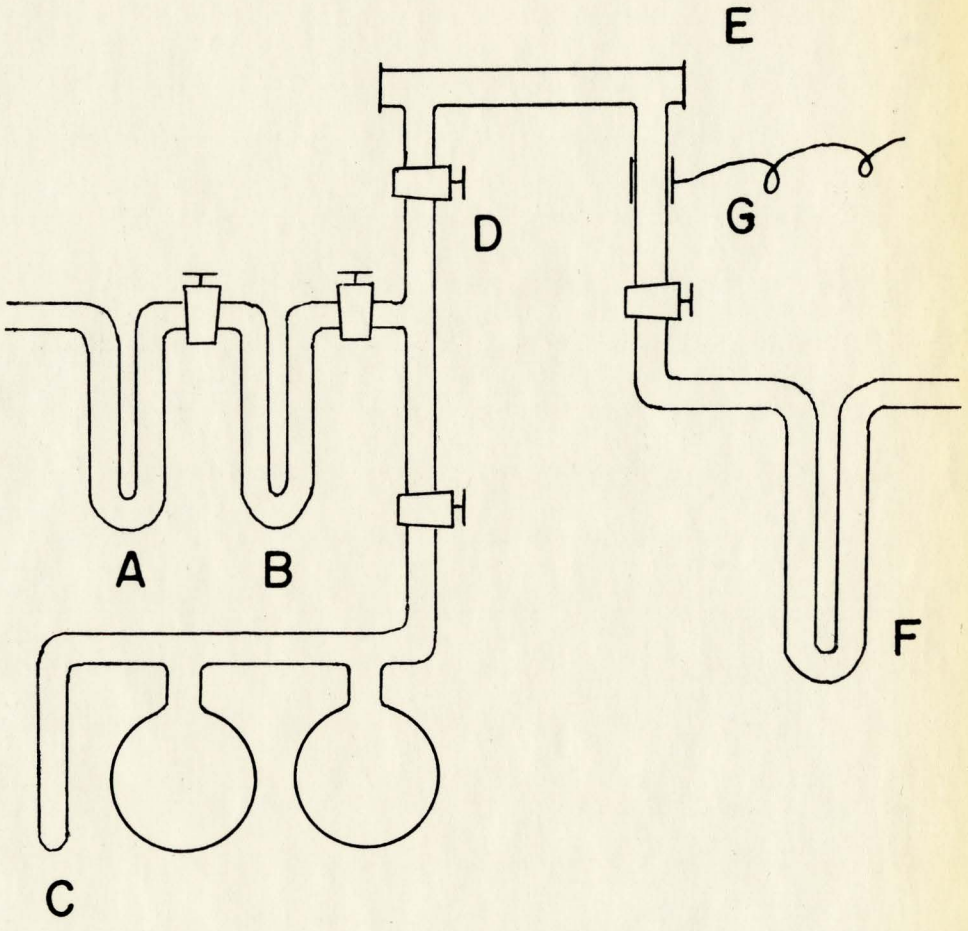

FIG. 8 THE EMISSION APPARATUS

attached to the end facing with the spectrograph slit, with picien wax. The streaming vapour was excited with a tesla coil operating at 300 kc/sec. whose probe touched the outlet side arm (g) of the emission cell. With the probe in this position, the impurity spectra which were invariably present were minimised. After passing from the emission cell, the vapour was collected in trap (f), which was maintained at liquid nitrogen temperature, thus protecting the fore-pump.

The spectra were recorded over a range of pressures and flow rates. At low gas pressures, the glow was observed to completely fill the discharge tube and to extend several feet into the auxiliary vacuum line. Under these conditions, the spectrum of this glow consisted mainly of the diatomic species, CO, C_2 and CH. At higher flow rates and pressures, the discharge was constricted into a narrow beam in the emission cell. Under these conditions, the propynal emission appeared with high intensity, while the impurity spectra were composed chiefly of CH and C_2 emission bands, the Herzberg and Angstrom systems of CO being extremely weak. The propynal spectrum appeared with maximum intensity when the gas pressures were set at the highest possible values which allowed the glow to be maintained; this was estimated to be approximately 0.5 mm.Hg. The emission spectra were photographed in the first order of the Bausch and Lomb 1.5 meter grating spectrograph. Slit widths of 60 microns were used, while the exposure times varied from 10 minutes to 2 hours, using Ilford FP3 film. Light of wave-length 1830 - 3600 Å was eliminated

by a 2 mm. thickness of Chance Bros. type OY10 filter. An iron arc reference spectrum was imposed on the film immediately before or after each exposure, for calibration purposes. The spectrum was microphotometered and calibrated by the methods described earlier.

CHAPTER 7

THE VIBRATIONAL ANALYSIS OF THE $^3A'' \leftarrow {}^1A'$ TRANSITION

I. A SURVEY OF THE ULTRA-VIOLET SPECTRUM OF PROPYNAL: The vapour spectrum of propynal from 8000 Å to 2000 Å is presented in Figure 9, which is a low resolution scan with the Spectracord. The spectra can be divided into three systems, namely, a weak absorption between 3800 Å and 3000 Å displaying a complex vibrational structure, a vibrationally discrete absorption in the region 2600 - 2100 Å, and an intense absorption continuum setting in at 2200 Å and extending beyond the low wave-length limit of the spectrophotometer. On the basis of the measured oscillator strength and frequency, Howe and Goldstein[3] assigned the near ultra-violet spectrum at 3800 Å to a $^1n_o \longrightarrow {}^1\pi^*$ transition in the carbonyl group. Although they extended their measurements down to 1900 Å, they failed to observe, however, the 2600 Å system.

When the spectrum was photographed with a Bausch and Lomb spectrograph at path lengths of 10 meters or greater, an additional absorption was detected in the 4100 Å region. From the weakness of this absorption, and the fact that the contours of these bands are different from those in the 3800 Å system, it seems reasonable to assign this spectrumto the corresponding singlet-triplet transition $^1n_o \longrightarrow {}^3\pi^*$. Bands in the spectrum of the intense blue-

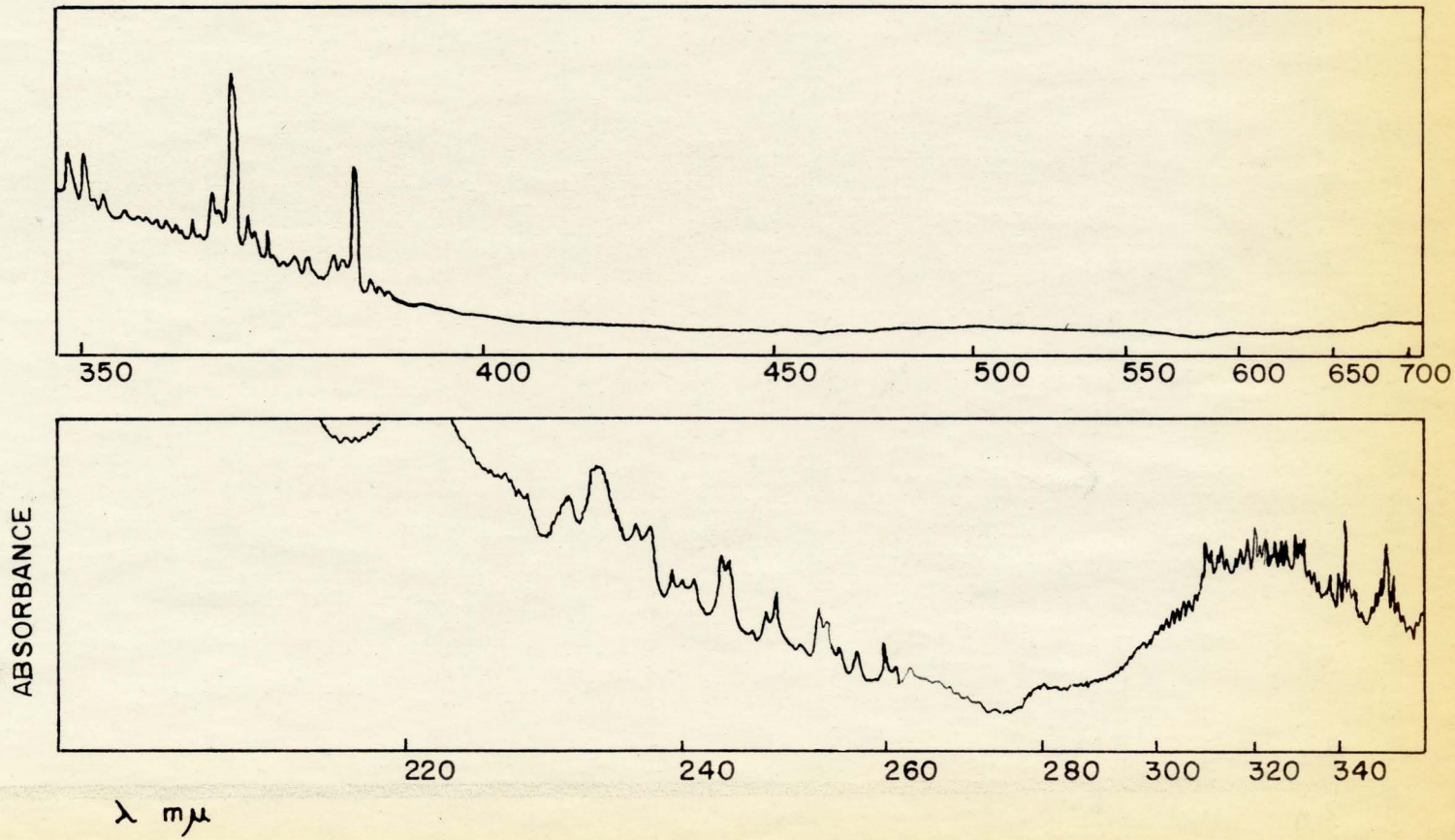

FIG. 9 THE U.V. SPECTRUM OF PROPYNAL

green emission resulting from the radio frequency excitation of streaming propynal vapour coincide with absorption bands in the 4100 Å region, as shown in Figure 10. The band at 4144 Å, which appears with high intensity in both the emission and absorption spectra, can at this stage be tentatively identified as the (0-0) origin band of the singlet-triplet transition. This assignment is confirmed by the vibrational and rotational analyses.

The system beginning at 3000 Å, while vibrationally sharp under the resolution of the Bausch and Lomb spectrograph, proved to be rotationally diffuse when photographed under high resolution. It was not examined further.

The spectrum at 3800 Å, assigned to the $^1n_o \leftarrow {}^1\pi^*$ transition was photographed in the first and second orders of the Ebert spectrograph. At a resolution of 300,000 the rotational line structure was well resolved, which is somewhat surprising for a molecule of this molecular weight. The (0-0) band at 3820 Å had a rotational structure which could be described by the prolate symmetric top equation (8.17), for perpendicular type bands, rather than equation (8.16) for parallel type bands. If it is assumed that the transition is allowed, the transition moment must then be directed out of the molecular plane, and from the arguments given in Chapter 5, it follows that the electronic symmetry of the excited state is A" and the transition is $^1A'' \leftarrow {}^1A'$. The weaker absorption with the electronic origin at 4144 Å results from the corresponding spin forbidden transition, $^3A'' \leftarrow {}^1A'$.

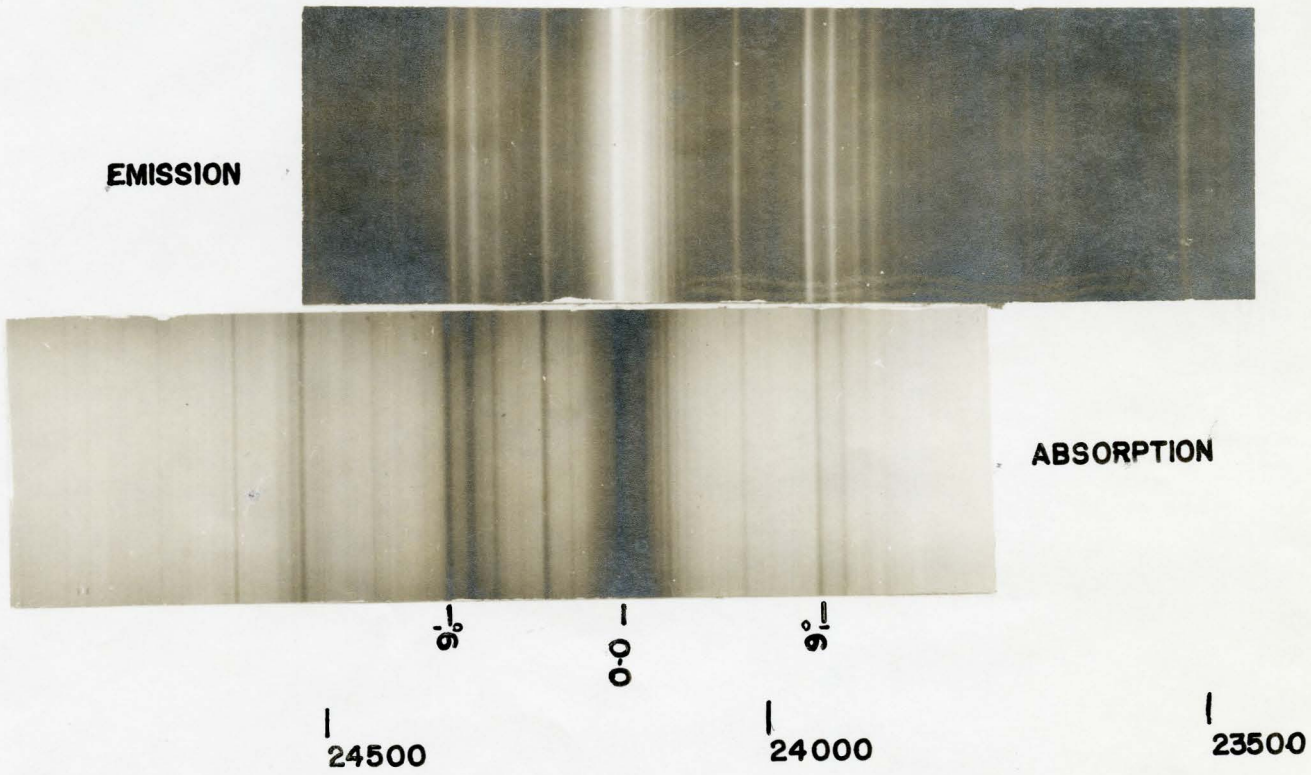

FIG. 10 THE EMISSION & ABSORPTION SPECTRA OF THE $^3A'' \leftarrow {}^1A'$ TRANSITION IN HC≡CCHO

It came to our notice at this stage in the investigation that a study of the $^1n_o \longrightarrow {}^1\pi^*$ transition in propynal was in progress at University College, The University of London, where Dr. J. H. Callomon was examining the rotational structure of the (0-0) band at 3820Å while Dr. J. C. D. Brand and Mr. J. K. G. Watson of the University of Glasgow, were assigning the vibrational structure. Since their programme of investigation of the singlet-singlet transition had advanced further than ours, it was agreed that we should shift our interest to the singlet-triplet transition which has an electronic origin at 4144 Å.

II. THE VIBRATIONAL ANALYSIS OF THE $^3A'' \leftarrow {}^1A'$ TRANSITION: The vibrational analysis of the singlet-triplet absorption spectrum is complicated by several factors. Most significant of these is that the intensity of the singlet-triplet absorption spectrum is very much weaker than the corresponding singlet-singlet spectrum. Since the separation between the electronic origins of the two spectra is only 1700 cm^{-1}, hot bands in the singlet-singlet absorption spectrum, that is bands resulting from transitions from vibrationally excited levels in the ground state, overlap and eventually obliterate the bands of the singlet-triplet absorption at shorter wave lengths. One method which has been used successfully in overcoming such interference is to cool the absorbing gas, and depopulate the vibrational levels in the ground state, and thereby reduce the intensity of the singlet-singlet hot bands in the singlet-triplet region. At temperatures sufficiently low to reduce interference from the singlet-

singlet hot bands, the vapour pressure of propynal is so reduced that the absorption bands of the singlet-triplet spectrum cannot be photographed even at path lengths up to 60 meters. Consequently, interference from the singlet-singlet system cannot be easily eliminated from the singlet-triplet spectrum.

The emission spectrum is the best place to begin a vibrational analysis of the singlet-triplet system, since some of the observed wave-number intervals should correspond to the wavenumbers of the infra-red and Raman bands. The analysis of the emission spectrum, aside from enabling the ground state frequencies to be determined with accuracy, should also yield those excited state frequencies which occur in fundamental, sequences or difference bands in the spectrum. For small changes in geometry on excitation, the emission and absorption spectra should bear a mirror image relationship to each other about the electronic origin, which should aid in the assignment of the absorption spectrum. (In actual fact, the analysis of the emission and the absorption spectra proceeded simultaneously, and the assignment of excited state frequencies presented in this section agrees with the analysis of the absorption spectrum given in the following section).

The vacuum wave numbers of the emission bands, which are presented in the first column of Table 7, are believed to be accurate to $\pm$ 2 cm^{-1}. The second column gives a rough measure of the intensity of each of the bands, obtained from a microdensitometer trace of the spectrum. The last column gives the assignment of the

TABLE 6

THE IMPURITY BANDS IN THE EMISSION SPECTRUM IN Å

CO ANGSTROM SYSTEM	6620	5610	4835
	6299	5399	4510
	6079	5198	4393
	5818	5016	4123
CO HERZBERG BANDS	5705	4661	3893
	5318	4380	3680
	4972	4124	
CH BANDS	4890	4025	4940
	4315	3889	4384
	4312	3628	3871
C_2 SWAN BANDS	4365	4678	4737
	4371	4684	5097
	4382	4697	5129
	4668	4715	
C_2 DESLANDRES AND D'AZAMBUKA BANDS	4102	4041	3852
	4068	4026	3825
H ATOMIC LINES	6562	4861	4340

TABLE 7

THE EMISSION BANDS OF THE $^3A'' \rightarrow {}^1A'$ TRANSITION

Wavenumber	Intensity	Notation	Assignment	
26,322.1	(vvvw)	$9'_0$	$\upsilon_0+\upsilon'_9$	(S)
26,141.6	(vvvw)	origin	υ_0	(S)
25,950.3	(vvvw)	C_2		
25,816.3	(vvvw)	CH		
25,678.8	(vvvw)	CH		
25,661	(vvvw)	CH		
25,642.2	(vvvw)	CH		
25,617.9	(vvvw)	CH		
25,593.6	(vvvw)	CH		
25,566.0	(vvvw)	CH		
25,528.3	(vvvw)	CH		
25,489.7	(vvvw)	CH		
25,446.5	(vvvw)	CH		
25,396.2	(vvvw)	CH		
25,343.7	(vvvw)	CH		
25,286.8	(vvvw)	CH		
24,575.6	(vvvw)	C_2		
24,477.7	(w)	4^0_1	$\upsilon_0-\upsilon''_4$	(S)
24,468.7	(mw)	4^0_1	$\upsilon_0-\upsilon''_4$	(S)
24,451.7	(vw)	4^0_1	$\upsilon_0-\upsilon''_4$	(S)

Wavenumber	Intensity	Notation	Assignment
24,438.6	(vvvw)	4_1^0	$\upsilon_0 - \upsilon_4''$
24,392.6	(vvvw)	$4_1^0\ 9_0'\ 12_1'$	$\upsilon - \upsilon_4'' + \upsilon_9' + \upsilon_{12}'$ (S) $- \upsilon_{12}''$
24,374.9	(w)	C_2	
24,309.9	(ms)	$9_0'$	$\upsilon_0 + \upsilon_9'$
24,285.4	(ms)	9_1^2	$\upsilon_0 + 2\upsilon_9' - \upsilon_9''$
24,260.1	(ms)	9_2^3	$\upsilon_0 + 3\upsilon_9' - 2\upsilon_9''$
24,238.1	(m)	9_3^4	$\upsilon_0 + 4\upsilon_9' - 3\upsilon_9''$
24,207.9	(ms)	$12_1'$	$\upsilon_0 + \upsilon_{12}' - \upsilon_{12}''$
24,180.8	(m)	$9_1'\ 12_1'$	$\upsilon_0 + \upsilon_9' - \upsilon_9'' + \upsilon_{12}' - \upsilon_{12}''$
24,127.8	(vs)	origin	υ_0
24,104.7	(s)	$9_1'$	$\upsilon_0 + \upsilon_9' - \upsilon_9''$
24,000.3	(ms)	$9_1^0\ 12_1'$	$\upsilon_0 - \upsilon_9'' + \upsilon_{12}' - \upsilon_{12}''$
23,974.3	(m)	$9_2'\ 12_1'$	$\upsilon_0 + \upsilon_9' - 2\upsilon_9'' + \upsilon_{12}' - \upsilon_{12}''$
23,923.3	(ms)	9_1^0	$\upsilon_0 - \upsilon_9''$
23,899.5	(ms)	$9_2'$	$\upsilon_0 + \upsilon_9' - 2\upsilon_9''$
23,874.1	(m)	9_3^2	$\upsilon_0 + 2\upsilon_9' - 3\upsilon_9''$
23,854.5	(m)	12_1^0	$\upsilon_0 - \upsilon_{12}''$
23,798.3	(vvw)	$9_2^0\ 12_1'$	$\upsilon_0 - 2\upsilon_9'' + \upsilon_{12}' - \upsilon_{12}'$
23,776.4	(vvw)	$9_3'\ 12_1'$	$\upsilon_0 + \upsilon_9' - 3\upsilon_9'' + \upsilon_{12}' - \upsilon_{12}''$
23,734.5	(vvvw)	CO^+	
23,718.8	(vw)	9_2^0	$\upsilon_0 - 2\upsilon_9''$
23,691.1	(vw)	$9_3'$	$\upsilon_0 + \upsilon_9' - 3\upsilon_9''$
23,664.2	(vw)	9_4^2	$\upsilon_0 + 2\upsilon_9' - 4\upsilon_9''$
23,649.2	(vvvw)	$9_1^0\ 12_1^0$	$\upsilon_0 - \upsilon_9'' - \upsilon_{12}''$

Wavenumber	Intensity	Notation	Assignment
23,636.2	(vvvw)	CH	
23,626.4	(vvvw)	CO^+	
23,593.3	(vvvw)	CH	
23,564.2	(vvvw)	CH	
23,530.7	(w)	10^1_1 (?)	$\upsilon_0 + \upsilon'_{10} - \upsilon''_{10}$
23,507.7	(vw)	8^0_1 (?)	$\upsilon_0 - \upsilon''_8$
23,491.9	(vw)	CH	
23,459.3	(vvw)	CH	
23,439.3	(vvvw)	CH	
23,426.0	(vvw)	CH	
23,390.8	(vvvw)	CH	
23,367.8	(vvvw)	CH	
23,359.4	(vw)	CH	
23,341.9	(vvvw)	CH	
23,323.8	(vw)	CH	
23,309.3	(vvw)	CH	
23,296.7	(vw)	CH	
23,291.6	(vw)	CH	
23,286.1	(vvw)	CH	
23,276.4	(vvw)	CH	
23,264.5	(vw)	CH	
23,254.9	(vvw)	CH	
23,245.3	(vvw)	CH	
23,235.7	(vvw)	CH	

Wavenumber	Intensity	Notation	Assignment
23,229.2	(vvw)	CH	
23,187.4	(w)	CH	
23,123.7	(vvw)	CH	
23,033.6	(vvw)	H (atomic)	
23,016.3	(vvvw)	CH	
22,992.7	(vvvw)	CH	
22,978.6	(vvvw)	CH	
22,968.6	(vvvw)	CH	
22,927.1	(vvvw)	CH	
22,906.8	(vvw)	C_2	
22,871.1	(vvw)	C_2	
22,791.5	(vvw)	$4_1^0\ 9_0^2$	$\upsilon_0 - \upsilon_4'' + 2\upsilon_9'$
22,776.1	(vvw)	$4_1^0\ 12_0'$	$\upsilon_0 - \upsilon_4'' + \upsilon_{12}'$
22,742.9	(vvw)	5_1^0	$\upsilon_0 - \upsilon_5''$
22,720.8	(vvw)	$5_1^0\ 9_1'$	$\upsilon_0 - \upsilon_5'' + \upsilon_9' - \upsilon_9''$
22,688.4	(vvw)	$4_1^0\ 9_0'\ 12_1'$	$\upsilon_0 - \upsilon_4'' + \upsilon_9' + \upsilon_{12}' - \upsilon_{12}''$
22,664.9	(vvw)	$4_1^0\ 9_1^2\ 12_1'$	$\upsilon_0 - \upsilon_4'' + 2\upsilon_9' - \upsilon_9'' + \upsilon_{12}' - \upsilon_{12}''$
22,613.2	(s)	$4_1^0\ 9_0'$	$\upsilon_0 - \upsilon_4'' + \upsilon_9'$
22,587.4	(s)	$4_1^0\ 9_1^2$	$\upsilon_0 - \upsilon_4'' + 2\upsilon_9' - \upsilon_9''$
22,560.5	(s)	$4_1^0\ 9_2^3$	$\upsilon_0 - \upsilon_4'' + 3\upsilon_9' - 2\upsilon_9''$
22,536.3	(ms)	$4_1^0\ 9_3^4$	$\upsilon_0 - \upsilon_4'' + 4\upsilon_9' - 3\upsilon_9''$
22,507.4	(s)	$4_1^0\ 12_1'$	$\upsilon_0 - \upsilon_4'' + \upsilon_{12}' - \upsilon_{12}''$
22,480.4	(ms)	$4_1^0\ 9_1'\ 12_1'$	$\upsilon_0 - \upsilon_4'' + \upsilon_9' - \upsilon_9'' + \upsilon_{12}' - \upsilon_{12}''$
22,430.4	(vvs)	4_1^0	$\upsilon_0 - \upsilon_4''$

Wavenumber	Intensity	Notation	Assignment
22,405.7	(vs)	$4_1^0\ 9_1'$	$\nu_0 - \nu_4'' + \nu_9' - \nu_9''$
22,308.8	(s)	$4_1^0\ 9_1^0\ 12_1'$	$\nu_0 - \nu_4'' - \nu_9'' + \nu_{12}' - \nu_{12}''$
22,283.8	(m)	$4_1^0\ 9_2'\ 12_1'$	$\nu_0 - \nu_4'' + \nu_9' - 2\nu_9'' + \nu_{12}' - \nu_{12}''$
22,225.6	(s)	$4_1^0\ 9_1^0$	$\nu_0 - \nu_4'' - \nu_9''$
22,200.2	(s)	$4_1^0\ 9_2'$	$\nu_0 - \nu_4'' + \nu_9' - 2\nu_9''$
22,173.9	(s)	$4_1^0\ 9_3^2$	$\nu_0 - \nu_4'' + 2\nu_9' - 3\nu_9''$
22,158.2	(s)	$4_1^0\ 12_1^0$	$\nu_0 - \nu_4'' - \nu_{12}''$
22,102.2	(w)	$4_1^0\ 9_2^0\ 12_1'$	$\nu_0 - \nu_4'' - 2\nu_9'' + \nu_{12}' - \nu_{12}''$
22,077.3	(w)	$4_1^0\ 9_3'\ 12_1'$	$\nu_0 - \nu_4'' + \nu_9' - 3\nu_9'' + \nu_{12}' - \nu_{12}''$
22,019.7	(w)	$4_1^0\ 9_2^0$	$\nu_0 - \nu_4'' - 2\nu_9''$
21,995.6	(w)	$4_1^0\ 9_3'$	$\nu_0 - \nu_4'' + \nu_9' - 3\nu_9''$
21,967.8	(vw)	$4_1^0\ 9_4^2$	$\nu_0 - \nu_4'' + 2\nu_9' - 4\nu_9''$
21,816.4	(vw)	$4_1^0\ 8_1^0$ (?)	$\nu_0 - \nu_4'' - \nu_8''$ ~~$- \nu_{10}''$~~
21,795.8	(vw)	$4_1^0\ 8_1^0\ 9_1'$ (?)	$\nu_0 - \nu_4'' - \nu_8'' + \nu_9' - \nu_9''$
21,495.9	(vw)	$4_1^0\ 6_1^0$	$\nu_0 - \nu_4'' - \nu_6''$
21,473.2	(vvvw)	$4_1^0\ 6_1^0\ 9_1'$	$\nu_0 - \nu_4'' - \nu_6'' + \nu_9' - \nu_9''$
21,381.8	(vvvw)	C_2	
21,370.9	(vw)	C_2	
21,363.0	(vvw)	C_2	
21,342.5	(vw)	C_2	
21,283.3	(vw)	C_2	
21,261.2	(vvvw)	2_1^0	$\nu_0 - \nu_2''$
21,237.5	(w)	C_2	
21,106.0	(vvw)	C_2	

Wavenumber	Intensity	Notation	Assignment
21,079.5	(w)	C_2	
21,049.3	(vvw)	$4_1^0\ 5_1^0$	$\upsilon_0 - \upsilon_4'' - \upsilon_5''$
20,937.9	(w)	$4_2^0\ 9_0^1$	$\upsilon_0 - 2\upsilon_4'' + \upsilon_9'$
20,912.5	(w)	$4_2^0\ 9_1^2$	$\upsilon_0 - 2\upsilon_4'' + 2\upsilon_9' - \upsilon_9''$
20,886.3	(vw)	$4_2^0\ 9_2^3$	$\upsilon_0 - 2\upsilon_4'' + 3\upsilon_9' - 2\upsilon_9''$
20,831.9	(w)	$4_2^0\ 12_1^1$	$\upsilon_0 - 2\upsilon_4'' + \upsilon_{12}' - \upsilon_{12}''$
20,756.8	(s)	4_2^0	$\upsilon_0 - 2\upsilon_4''$
20,736.4	(ms)	$4_2^0\ 9_1^1$	$\upsilon_0 - 2\upsilon_4'' + \upsilon_9' - \upsilon_9''$
20,640.2	(w)	$4_2^0\ 9_1^0\ 12_1^1$	$\upsilon_0 - 2\upsilon_4'' - \upsilon_9'' + \upsilon_{12}' - \upsilon_{12}''$
20,567.4	(w)	H atomic	
20,553.5	(m)	$4_2^0\ 9_1^0$	$\upsilon_0 - 2\upsilon_4'' - \upsilon_9''$
20,527.5	(w)	$4_2^0\ 9_2^1$	$\upsilon_0 - 2\upsilon_4'' + \upsilon_9' - 2\upsilon_9''$
20,500.1	(w)	$4_2^0\ 9_3^2$	$\upsilon_0 - 2\upsilon_4'' + 2\upsilon_9' - 3\upsilon_9''$
20,487.1	(w)	$4_2^0\ 12_1^0$	$\upsilon_0 - 2\upsilon_4'' - \upsilon_{12}''$
20,467.2	(w)	$4_2^0\ 9_1^1\ 12_1^0$	$\upsilon_0 - 2\upsilon_4'' + \upsilon_9' - \upsilon_9'' - \upsilon_{12}''$
20,346.6	(vvw)	$4_2^0\ 9_2^0$	$\upsilon_0 - 2\upsilon_4'' - 2\upsilon_9''$
20,150.54	(vvvw)	$4_2^0\ 8_1^0$	$\upsilon_0 - 2\upsilon_4'' - \upsilon_8''$
20,126.53	(vvvw)	$4_2^0\ 8_1^0\ 9_1^1$	$\upsilon_0 - 2\upsilon_4'' - \upsilon_8'' + \upsilon_9' - \upsilon_9''$
19,830.2	(vvvw)	C_2	
19,503.4	(vvw)	C_2	
19,494.3	(vw)	C_2	
19,357.7	(m)	C_2	
19,284.6	(vw)	$4_3^0\ 9_1^0$	$\upsilon_0 - 3\upsilon_4'' - \upsilon_9''$
19,258.2	(vw)	$4_3^0\ 9_2^1$	$\upsilon_0 - 3\upsilon_4'' + \upsilon_9' - 2\upsilon_9''$

Wavenumber	Intensity	Notation	Assignment
19,235.1	(vw)	CO	
19,176.7	(vw)	$4_3^0\ 12_1^1$	$\nu_0 - 3\nu_4'' + \nu_{12}' - \nu_{12}''$
19,102.7	(s)	4_3^0	$\nu_0 - 3\nu_4''$
19,197.9	(ms)	$4_3^0\ 9_1^1$	$\nu_0 - 3\nu_4'' + \nu_9' - \nu_9''$
19,201.5	(vw)	$4_3^0\ 9_1^0\ 12_1^1$	$\nu_0 - 3\nu_4'' - \nu_9'' + \nu_{12}' - \nu_{12}''$

* The symbol (S) denotes bands assigned to the singlet-singlet transition.

vibrational bands in terms of the normal modes used in the vibrational analysis of the ground state, presented in Chapter 4, while the third column is an abbreviated nomenclature that is used to identify the vibrational bands in Figures 11, 12 and 13. In this notation, the normal vibration is labelled according to its number in Table 5, and is followed by a sbuscript n" and a superscript n', which identify the vibrational quanta excited in the electronic ground and excited states respectively. Combination or difference bands are designated as products of the normal vibrations involved.

Before discussing the analysis of the emission spectrum, we must account for impurity bands in the spectrum that are due to the emission by molecular fragments resulting from the decomposition of propynal in the electrical discharge. Certain bands could be identified as arising from impurities because of their variation in intensity with respect to the propynal bands, under different conditions of gas pressure and excitation. These impurity bands were identified from Pearce and Gaydon[20], and are tabulated in Table 6. Under the conditions of high vapour pressure of propynal and fast flow rate through the discharge tube, it was possible to eliminate almost completely the Herzberg and Ångstrom bands of carbon monoxide from the spectrum. On the other hand, the spectra resulting from C_2 and CH molecules could not be eliminated as impurities by changing the conditions of excitation.

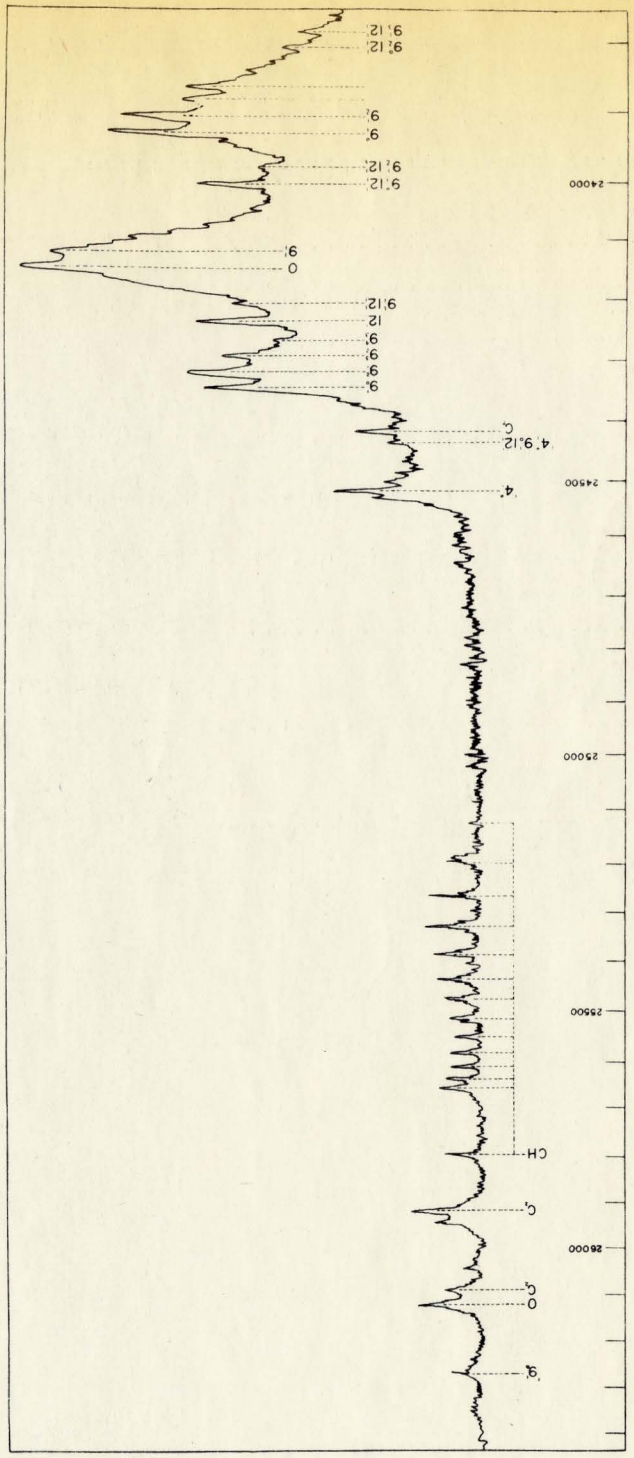

FIG. 11 THE EMISSION SPECTRUM OF HC≡CCHO

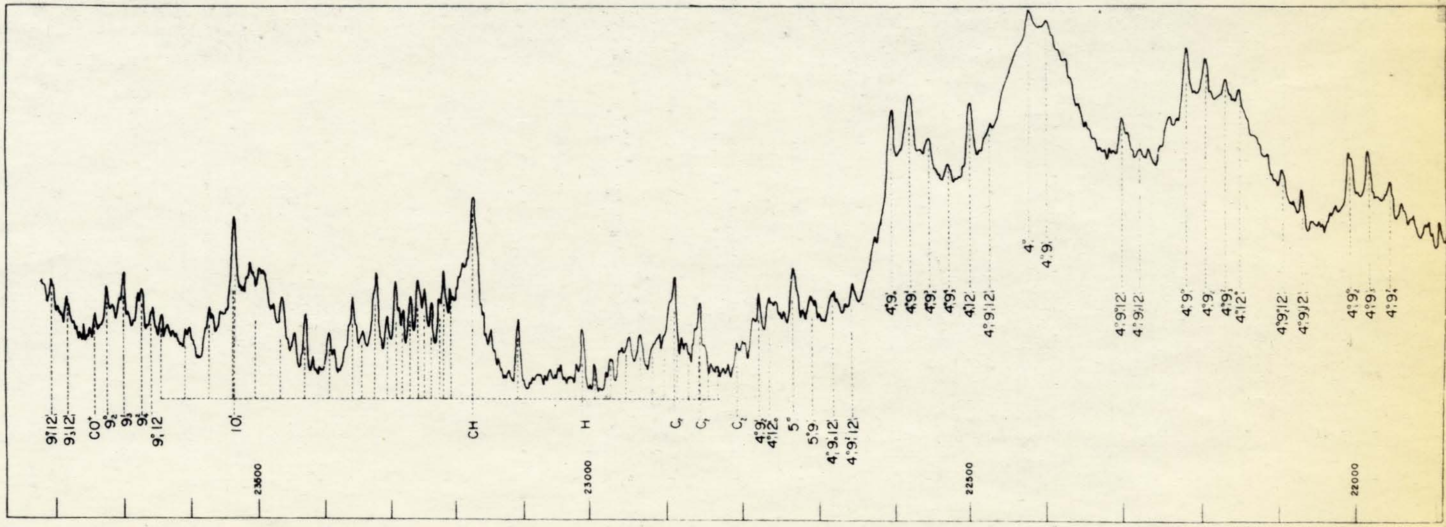

FIG. 12 THE EMISSION SPECTRUM OF HC≡CCHO

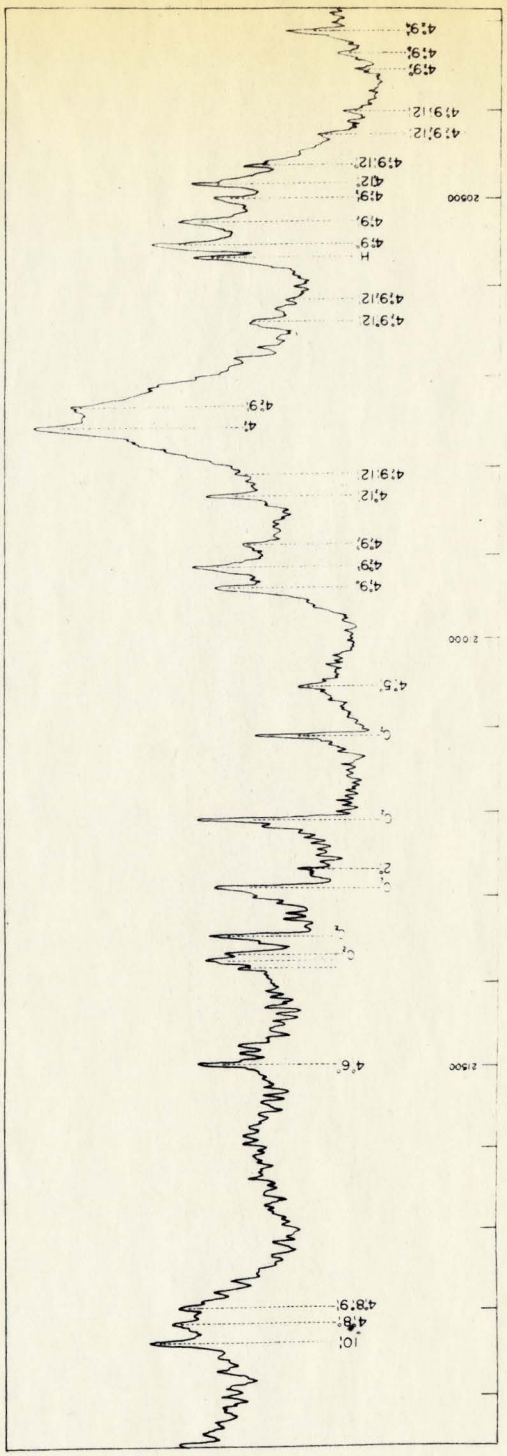

FIG. 13 THE EMISSION SPECTRUM OF HC≡CCHO

In the 3800 - 4000 Å region, lie a number of bands which can be identified as arising from diatomic impurities. Weak bands appearing at 26,322, 26,141 and 24,468 cm^{-1} cannot be ascribed to impurities, nor can they be classified in the vibrational scheme of the singlet-triplet analysis. Brand, Callomon and Watson[21] in their analysis of the singlet-singlet absorption spectrum have found bands at these wavenumbers which they were able to assign in their vibrational scheme. Therefore, it seems reasonable to assign the observed weak emission bands at these wavenumbers to the singlet system. These bands are identified as singlet bands on the first page of Table 7.

As illustrated in Figures 11, 12 and 13, the main feature of the emission spectrum is an intense progression which originates at 24,127 cm^{-1} and extends to the red with frequency intervals diminishing from 1697 cm^{-1} to 1654 cm^{-1} over the first three quanta. The interval is assigned to the carbonyl stretching mode ν''_4, which appears at 1692 cm^{-1} in the infra-red spectrum.

A set of weaker bands appearing at either side of the origin band form a pattern which is repeated about each member of the carbonyl progression. These bands are too numerous to be assigned to fundamentals, sequences or overtones of a single mode, and are ascribed to various combinations of the low frequency modes ν_9 and ν_{12} in the ground and excited states. Nearly all of the emission bands are accompanied by bands extending to the red with frequency intervals of 25 cm^{-1}. These satellite bands are assigned to sequences arising from transitions between vibrationally excited levels in the

ground and excited electronic states. Wavenumber intervals of 204 cm^{-1} and 182 cm^{-1} between the electronic origin and intense vibrational bands which lie to the red and blue of the origin respectively, are assigned to the fundamental frequencies of this mode in the ground and excited electronic states. Since the fundamental and sequence bands of this mode have the same band contour, they have the same polarisation. They are therefore assigned to the in-plane bending mode of the CCC skeleton υ_9. The assignment of υ''_9 to the wavenumber interval of 204 cm^{-1} does not agree with the Raman analysis which assigned the diffuse band at 261 cm^{-1} to this mode on the basis of its depolarisation. As the contours of the vibrational bands are generally a more reliable method for determining the vibrational symmetry, than are the depolarisations of the Raman lines, it is necessary to reverse the Raman assignment.

Bands appear at 80 cm^{-1} to the blue of both the origin and carbonyl progression bands. These are assigned as sequence bands involving excitation of one quantum of the υ_{12} vibration in the ground and excited state. This frequency appears as a one quantum addition to the ground state. Our revised Raman data predicts the band $\upsilon_o - \upsilon''_{12}$ to lie at 261 cm^{-1} to the red of the origin. A band does not appear here, but an intense peak is located at 273 cm^{-1} to the red of the origin to which this is assigned. This discrepancy is believed to be caused by head formation within the band and the Raman frequency of 161 cm^{-1} is preferred for the υ''_{12} mode. The assignment then gives a frequency of 341 cm^{-1} to the out-of-plane

bending mode ν'_{12}. Over 80% of the vibrational bands in the electronic emission spectrum can be assigned to the activity of three vibrations $\upsilon''_4, \upsilon''_9$ and υ''_{12} in the ground and the vibrations υ'_9 and υ'_{12} in the excited states.

No excited state vibrations of large wavenumbers are active in the emission spectrum, which indicates that the molecule in the electronically excited state comes more or less into thermal equilibrium with its surroundings before emitting radiation. Under these conditions, we should only expect low frequency excited state vibrational modes, such as υ'_9 and υ'_{12}, to be active in the spectrum, as is observed to be the case. These skeletal modes should be approximately the same in both the singlet and triplet excited states; and our values of 182 and 341 cm^{-1} for υ'_9 and υ'_{12}, are close to Brand, Callomon and Watson's[21] corresponding values of 189 cm^{-1} and 345 cm^{-1} for the singlet $^1A''$ excited state.

By use of the ground state frequencies of the CHO, CC, and CCO modes, $\upsilon''_5, \upsilon''_6$ and υ''_8, which were obtained from the analysis of the infra-red and Raman spectra, it was possible to identify bands in the emission spectrum resulting from transitions in which these vibrations were active. A weak prominence appears at 1385 cm^{-1} to the red of the origin band, and is assigned to the CHO in-plane bending mode υ''_5. Analogous bands with the same interval and intensity are associated with the other members of the carbonyl progression. The $\upsilon_o - \upsilon''_6$ band is overlapped by an emission band at 23,187 cm^{-1}

due to the CH radical; however, it is possible to find the ν''_6 vibration in combination with the second and third harmonics of the ν''_4 mode. A broad hump appearing at 620 cm^{-1} to the red of the electronic origin may be tentatively assigned to the $\nu_o - \nu''_8$ band.

Although the infra-red and Raman spectra indicate that the CHO mode ν''_{10} has a vibrational frequency of 990 cm^{-1}, the region about 23,140 cm^{-1} in which $\nu_o - \nu''_{10}$ should appear shows no bands of any appreciable intensity. Since the ν''_{10} vibrational coordinate involves motion of the carbonyl group it might be expected to be strongly active in the spectrum. Additional bands appear at 597 cm^{-1} to the red of each member of the carbonyl progression. These are difficult to fit into any vibrational scheme involving the ground state fundamentals combined with reasonable values for the excited state fundamentals. This frequency interval possibly represents a sequence in which one quantum of ν_{10} is active in the ground and excited states. This assignment would require a large drop in frequency for this vibrational mode from 990 to 393 cm^{-1}, on excitation into the triplet state; such a drop has been observed for this frequency in the singlet excited state.

III. THE ABSORPTION SPECTRUM LOW RESOLUTION: A section of the absorption spectrum of normal propynal HC≡CCHO is reproduced in figure 10, (the absorption spectra appearing as dark bands on a light background). The wavenumbers of the observed bands are collected in Table 8, along with the intensities and the vibrational assignment of the bands. As shown in Figure 10, bands of the emission and absorption spectra coincide in the 4100 Å region. The assignment of

TABLE 8

THE ABSORPTION BANDS OF THE $^3A'' \rightarrow {}^1A'$ TRANSITION

Wavenumber	Intensity	Notation	Assignment
23,901.2	(vvvw)	$9_2'$	$\upsilon_0 + \upsilon_9' - 2\upsilon_9''$
23,925.2	(vvw)	9_1^0	$\upsilon^0 - \upsilon_9''$
24,000.9	(vvvw)	$9_1^0\ 12_1'$	$\upsilon_0 - \upsilon_9'' + \upsilon_{12}' - \upsilon_{12}''$
24,104.8	(ms)	$9_1'$	$\upsilon_0 + \upsilon_9' - \upsilon_9''$
24,125.3	(vs)	origin	υ_0
24,180.9	(vvvw)	$9_1'\ 12_1'$	$\upsilon_0 + \upsilon_9' - \upsilon_9'' + \upsilon_{12}' - \upsilon_{12}''$
24,208.5	(vw)	$12_1'$	$\upsilon_0 + \upsilon_{12}' - \upsilon_{12}''$
24,259.8	(vw)	9_2^3	$\upsilon_0 + 3\upsilon_9' - 2\upsilon_9''$
24,286.5	(m)	9_1^2	$\upsilon_0 + 2\upsilon_9' - \upsilon_9''$
24,310.4	(m)	$9_0'$	$\upsilon_0 + \upsilon_9'$
24,389.7	(vvvw)	$9_0'\ 12_1'$	$\upsilon_0 + \upsilon_9' + \upsilon_{12}' - \upsilon_{12}''$
24,489.3	(vvvw)	9_0^2	$\upsilon_0 + 2\upsilon_9'$
25,187.9	(vw)	$4_0'\ 9_3^2$	$\upsilon_0 + \upsilon_4' + 2\upsilon_9' - 3\upsilon_9''$
25,216.7	(vw)	$4_0'\ 9_2'$	$\upsilon_0 + \upsilon_4' + \upsilon_9' - 2\upsilon_9''$
25,243.2	(vw)	$4_0'\ 9_1^0$	$\upsilon_0 + \upsilon_4' - \upsilon_9''$
25,450.8	(s)	$4_0'$	$\upsilon_0 + \upsilon_4'$

the absorption bands then follows from the assignment of the emission bands. At shorter wave lengths the spectrum is overlapped by hot bands arising from the $^1n_o \longrightarrow {}^1\pi^*$ transition. The carbonyl mode ν'_4 may be distinguished on the absorption continuum as an intense band at 25,450 cm^{-1} along with the combination $\nu_o + \nu'_4 - \upsilon''_9$ at 25,243 cm^{-1}.

CHAPTER 8

THE THEORY OF THE ROTATIONAL STRUCTURES OF SINGLET-TRIPLET TRANSITIONS

I. THE MOMENTS OF INERTIA: The rotational motions of a molecule are dynamically balanced about three mutually perpendicular axes, (the principal axes) which pass through its centre of mass. These are customarily labelled a, b, and c in such a way that the moments of inertia (the principal moments of inertia), increase in the order $I_a < I_b < I_c$. The moment of inertia of a rigid molecule about one of the principal axes is given by

$$I = \sum_i m_i r_i^2 \qquad (8.1)$$

where r_i is the perpendicular distance from the axis, m_i the mass, and the summation taken over all nuclei. The directions of these axes may be obvious in molecules with high symmetry, since they must coincide with symmetry axes or lie in symmetry planes, and the moments of inertia in such cases can be obtained directly from equation (8.1); otherwise, they must be calculated by the method of Hirschfelder[22].

Molecules may be grouped into five categories according to the relationships between the principal moments of inertia.

i	$I_a = I_b = I_c$	- spherical top
ii	$I_a = 0, I_b = I_c$	- linear top
iii	$I_a < I_b = I_c$	- prolate symmetric top

iv $I_a = I_b < I_c$ - oblate symmetric top

v $I_a < I_b < I_c$ - asymmetric top

II. ROTATIONAL ENERGY LEVELS: The total angular momentum of a rigid molecule may be represented classically by a vector $\underline{P}$. At each instant during molecular rotation, $\underline{P}^2$ may be resolved into components of angular momentum $\underline{P}_a$, $\underline{P}_b$ and $\underline{P}_c$ along the principal axes of the molecule, such that

$$\underline{P}^2 = \underline{P}_a^2 + \underline{P}_b^2 + \underline{P}_c^2 \qquad (8.2)$$

The classical energy of rotation is

$$E = \frac{\underline{P}_a^2}{2I_a} + \frac{\underline{P}_b^2}{2I_b} + \frac{\underline{P}_c^2}{2I_c} \qquad (8.3)$$

where I_a, I_b and I_c are the principal moments of inertia.

For the prolate symmetric top, case (iii), the angular momentum $\underline{P}_a$ about the a axis is conserved. From the fact that $I_b = I_c$, and from equations (8.2) and (8.3)

$$E = \frac{\underline{P}^2}{2I_b} + \underline{P}_a^2\left[\frac{(1}{2I_a} - \frac{1)}{2I_b}\right] \qquad (8.4)$$

According to quantum theory the rotational energy levels are quantised and are restricted to certain values. The square of the total angular momentum $\underline{P}^2$ is quantised and must equal $J(J+1)h^2/4\pi^2$, where J is the quantum number and may take integral values. Similarly, the component of the angular momentum, $\underline{P}_a$, along the top axis is quantised so that $\underline{P}_a^2 = K^2h^2/4\pi^2$ where K is the quantum number. The energy of the prolate symmetric top is given by

$$E(J,K)=\frac{J(J+1)h^2}{8\pi^2 I_b} + \frac{h^2}{8\pi^2}\left[\frac{1}{I_c} - \frac{1}{I_b}\right]K^2 \qquad (8.5)$$

If the rotational constants are defined as $A = h^2/8\pi^2 cI_a$ and $B = h^2/8\pi^2 cI_b$, the rotational term values (cm-1) become

$$F(J,K) = BJ(J+1) + (A-B)K^2 \qquad (8.6)$$

Since K represents a component of J along the top axis, K cannot be greater than J and may have possible values

$$K = 0,1 \ldots J \qquad (8.7)$$

Each level with a given value of $K > 0$ is doubly degenerate.

The energy levels for a rigid oblate top $I_a = I_b < I_c$ are given by

$$F(J,K) = BJ(J+1) + (C-B)K^2 \qquad (8.8)$$

for fixed J; the energy, therefore, increases as K decreases, whereas, for the prolate top the energy increases as K increases.

In the asymmetric top, the two-fold degeneracy of levels with the same value of K is removed, and for each value of J there are 2J+1 different energy levels. For an asymmetric top, the quantum number K is not defined, since the angular momentum about the a axis is not conserved, but if we suppose B to be increased gradually from B = C (prolate top) to B = A (oblate top), there should be a continuous change in energy of the levels. The lowest level for a given J in the near-prolate top is the lowest level for the same J in the near-oblate symmetric top and so on. Thus, the level J = 1, K = 0 of the prolate symmetric top must become the lower of

the two components into which the J = 1, K = 1 level of the oblate symmetric top split. Herzberg,[23] page 45, shows the correlation diagram illustrating this point. Each rotational level may be identified by its J value and by the prolate and oblate K values, K_{-1} and K_1 to which it correlates in these limiting cases. Thus, the level may be designated as $J_{K_{-1}\,K_{+1}}$

Although K is not strictly defined for an asymmetric top, for a near-prolate top we may still use equation (8.5) providing the rotational constant B is replaced by the effective rotational constant $\bar{B} = (B+C)/2$. A convenient parameter that measures the asymmetry is $\kappa = (2B-A-C)/(A-C)$, which becomes -1 for a prolate symmetric top and +1 for an oblate symmetric top and varies between these two values for asymmetric tops. For propynal, $\kappa = -0.989$ in the ground state and $\kappa = -.984$ in the triplet excited state.

Corrections are also needed to equation (8.5) for the effect of centrifugal distortion. The energy levels of a non-rigid prolate symmetric top are given by

$$F(J,K)=BJ(J+1)+(A-B)K^2-D_J J^2(J+1)^2-D_{JK}J(J+1)K^2-D_K K^4 \qquad (8.9)$$

For a molecule which is a symmetric top in its ground and excited states, the rotational selection rules for a transition directed normal to the a axis are

$$\Delta J = 0, \pm 1 \quad \text{- perpendicular bands} \qquad (8.10)$$
$$\Delta K = \pm 1$$

and when the transition moment is directed parallel to the top axis,

$$\left.\begin{array}{l}\Delta J = 0, \pm 1 \\ \Delta K = 0\end{array}\right\} \text{ - parallel bands} \qquad (8.11)$$

The wavenumbers of the rotational lines, in a spectral band are given by the difference between the term values in the ground and excited states as

$$\nu = \nu_o + \bar{B}'J'(J'+1) - \bar{B}''J''(J''+1) + (A' - \bar{B}')K^2 - (A'' - \bar{B}'')K^2 \qquad (8.12)$$

where the double primes are used to denote the ground state and the single primes the excited state.

Transitions which occur between states with fixed values of K' and K", accompanied by the changes -1, 0, + 1 in the total quantum number J, result in the formation of P, Q and R branches.

P branch

$$J' = J - 1, \qquad J'' = J$$

$$\nu = \nu_o + (\bar{B}' - \bar{B}'')J^2 - (\bar{B}' + \bar{B}'')J + \nu_k \qquad (8.13)$$

Q branch

$$J' = J, \qquad J'' = J$$

$$\nu = \nu_o + (\bar{B}' - \bar{B}'')J^2 + (\bar{B}' - \bar{B}'')J + \nu_k \qquad (8.14)$$

R branch

$$J' = J + 1 \qquad J'' = J$$

$$\nu = \nu_o + (\bar{B}' - \bar{B}'')J^2 + (3\bar{B}' - \bar{B}'')J + 2\bar{B}' + \nu_k \qquad (8.15)$$

These branches form a series of sub-bands when the quantum number K changes by $0, \pm 1$. Each of these sub-bands may be referred to an origin, which is where the hypothetical J" = 0, J' = 0 line would occur. The frequencies for these sub-band origins are given by the equation

$$\nu_k = ((A' - \bar{B}') - (A'' - B''))K^2 \qquad (8.16)$$

for a parallel type band, and for the perpendicular band the origins are given by

$$\upsilon_k = (A'-\bar{B}') \pm 2(A'-\bar{B}')K + ((A'-\bar{B}')-(A''-\bar{B}''))K^2 \qquad (8.17)$$

This approximation is valid for large values of the quantum number K. Propynal is a near prolate symmetric top in its electronic ground and excited states that we are considering, and the equations developed above for the rotational line frequencies were used in the analysis of rotational sub-bands with $K > 3$.

III. ROTATIONAL ENERGY LEVELS IN THE $^3A''$ STATE: In the ground state of most non-linear polyatomic molecules, the total angular momentum is a result of rotational motions of the nuclei about the principal axes. The unpairing of the spins of two electrons in the $^3A''$ state of propynal introduces additional angular momentum associated with the spin and orbital angular momenta of the electrons, besides the angular momentum due to molecular rotation of the nuclei about the principal axes. To describe the rotational energy levels in this state, additional terms have to be introduced into the rotor energy expression to account for the ineraction between these momenta.

The origin of the electronic angular momentum, and the spin angular momentum is now considered using the vector model. In a system composed of a single electron rotating in the central force field of a single nucleus, the angular momentum of the electron may be represented by the vector $\underline{l}$, which, neglecting the effect of electron spin, is a well defined constant of the motion. Besides this

orbital motion, the electron spins on an axis through its centre of mass with angular momentum represented by the vector $\underline{s}$. Because of the orbital motion of the electron of charge e in the radial electric field of the nucleus, there will be a magnetic field at the electron normal to the plane of the orbit. In this field, the magnetic moment associated with the spinning electron, like a small magnetic top, undergoes a Larmor precession about the field direction. The magnetic moment of the electron can then align itself either parallel or antiparallel to the magnetic field. When the magnetic moment is aligned in the field direction, the spin angular moment is directed antiparallel to the orbital angular momentum, and the total angular momentum $\underline{j} = \underline{l} - \underline{s}$. When the spin and orbital angular momenta are parallel to each other, $\underline{j} = \underline{l} + \underline{s}$, and the magnetic moment is opposed to the magnetic field. Since the total energy of the system is lower when the spin magnetic moment is aligned in the direction of the field, and higher when it is opposed to the field direction, the effect of spin angular momentum is to split the electronic state into two components, the lower energy level of the doublet $\underline{l} - \underline{s}$ and the higher level, $\underline{l} + \underline{s}$. The splitting between the two states in the electronic doublet is a function of the magnitude of spin-orbit coupling, which is a measure of the strength of the magnetic field at the electron.

In a polyatomic molecule, the spherical symmetry of the electric field which exists in an atom is destroyed. As a result, the electronic angular momentum, and the rotational angular

momentum are not conserved. The total angular momentum, excluding the electronic spin angular momentum, however, is approximately a constant of the motion about a space fixed axis.

In the vector model, the electronic angular momentum is represented by the vector $\underline{L}$, and the rotational angular momentum by $\underline{R}$. The resultant $\underline{N} = \underline{R} + \underline{L}$ is referred to as the orbital angular momentum vector. The component of $\underline{N}$ along the top axis, for a symmetric top, is represented by the vector $\underline{K}$. The total angular momentum vector $\underline{J}$ is then the vector sum of $\underline{N}$ and $\underline{S}$. When there is more than one unpaired electron, the spin angular momenta of the individual electrons couple together; the sum of the vectors representing the spin angular momenta is denoted by $\underline{S}$. The resultant spin vector $\underline{S}$ and the orbital-rotational vector $\underline{N}$ can only add together to give the total angular momentum vector $\underline{J}$ in accordance with the following relation between the quantum numbers defined by $J = (N+S), (N+S-1) \ldots (N-S)$. Because the energy corresponding to each of these values is different, each state with given values of S and N is split into 2S+1 components.

Henderson and Van Vleck[24] and Henderson[25] have derived an expression for this splitting of the rotational levels in asymmetric rotor molecules having spin angular momentum. This theory has been applied to the rotational structure of the singlet-triplet bands in formaldehyde by Robinson and DiGiorgio[26,27]. Since formaldehyde is very close to a symmetric top, the energy correction terms arising from the spin angular momentum were used by these authors only in the prolate symmetric limit. The treatment used by Robinson and DiGiorgio

may be adopted in this investigation, since propynal is also almost a symmetric top in the ground state, and is not expected to be appreciably more asymmetric in the excited state.

In the $^3A''$ state of propynal the magnitude of the total spin angular momentum $\underline{S}$ is equal to one (in units of $h/2\pi$). The total angular momentum $\underline{J}$ can have three values, $\underline{N}+1$, $\underline{N}$, and $\underline{N}-1$ corresponding to each of the three spin components of the $^3A''$ state. From the equations of Henderson and Van Vleck the rotational term values, F_1, F_2 and F_3, (the subscripts 1, 2 and 3 corresponding to $\underline{J} = \underline{N}+1$, $\underline{J} = \underline{N}$ and $\underline{J} = \underline{N}-1$ respectively) for each of the three members of the multiplet are

$$F_1(NK) = \bar{B}N(N+1) + (A-\bar{B})K^2 + \left[\frac{\lambda K^2}{N(N+1)} + \mu\right] 2N + \left[\frac{\lambda' K^2}{N(N+1)} + \mu'\right] \frac{N(N-\frac{1}{2})}{(2N-1)(2N+3)} \quad (8.18)$$

$$F_2(NK) = \bar{B}N(N+1) + (A-\bar{B})K^2 + \left[\frac{\lambda K^2}{N(N+1)} + \mu\right](-2) + \left[\frac{\lambda' K^2}{N(N+1)} + \mu'\right] \frac{3/2 - 2N(N+1)}{(2N-1)(2N+3)} \quad (8.19)$$

$$F_3(NK) = \bar{B}N(N+1) + (A-\bar{B})K^2 + \left[\frac{\lambda K^2}{N(N+1)} + \mu\right](-2)(N+1) + \left[\frac{\lambda' K^2}{N(N+1)} + \mu'\right] \frac{(N+1)(N+3/2)}{(2N-1)(2N+3)} \quad (8.20)$$

where λ, λ', μ, and μ', are parameters which describe the magnetic interaction between the angular momenta. These are not the fundamental coupling constants, although they can be related to the electric dipole and pseudoquadrupole constants by expression given by Robinson and DiGiorgio.

The corrections due to interaction between the momenta are small, and can be ignored to a first approximation. The frequencies for the rotational lines may be obtained as the difference between the term values for the ground and excited states, $F'(N',K')-F''(N'',K'')$.

In the ground electronic state of propynal the spins of the electrons are paired and the spin angular momentum is equal to zero. The orbital-rotational angular momentum and the total angular momentum are equivalent, and the quantum number J" and N" are identical. Disregarding the spin-orbit correction terms in equations (8.18), (8.19) and (8.20), the term values for the ground and excited states are given by

$$F(N,K) = \bar{B}N(N+1) + (A-\bar{B})K^2 \qquad (8.21)$$

The frequencies of the spectral lines from the differences between the term values are,

<u>J' = N'+1</u>

P_1 branch $\quad N' = N-2, \quad N'' = N$

$$\nu = \nu_o + (\bar{B}'-\bar{B}'')N^2 - (3\bar{B}'+\bar{B}'')N + 2\bar{B}' + \nu_k \qquad (8.22)$$

Q_1 branch $\quad N' = N-1, \quad N'' = N$

$$\nu = \nu_o + (\bar{B}'-\bar{B}'')N^2 - (\bar{B}'+\bar{B}'')N + \nu_k \qquad (8.23)$$

R_1 branch $\quad N' = N \qquad N'' = N$

$$\nu = \nu_o + (\bar{B}'-\bar{B}'')N^2 + (\bar{B}'-\bar{B}'')N + \nu_k \qquad (8.24)$$

<u>J' = N'</u>

P_2 branch $\quad N' = N-1, \quad N'' = N$

$$\nu = \nu_o + (\bar{B}'-\bar{B}'')N^2 - (\bar{B}'+\bar{B}'')N + \nu_k \qquad (8.25)$$

Q_2 branch $\quad N' = N \qquad N'' = N$

$$\nu = \nu_o + (\bar{B}'-\bar{B}'')N^2 + (\bar{B}'-\bar{B}'')N + \nu_k \qquad (8.26)$$

R_2 branch $\quad N' = N+1, \quad N'' = N$

$$\nu = \nu_o + (\bar{B}'-\bar{B}'')N^2 + (3\bar{B}'-\bar{B}'')N + 2\bar{B}' + \nu_k \qquad (8.27)$$

$\underline{J' = N' - 1}$

P_3 branch $\quad N' = N, \quad N'' = N$

$$\nu = \nu_o + (\bar{B}' - \bar{B}'')N^2 + (\bar{B}' - \bar{B}'')N + \nu_k \qquad (8.28)$$

Q_3 $\quad N' = N + 1, \quad N'' = N$

$$\nu = \nu_o + (\bar{B}' - \bar{B}'')N^2 + (3\bar{B}' - \bar{B}'')N + 2\bar{B}' + \nu_k \qquad (8.29)$$

R_3 branch $\quad N' = N + 2, \quad N'' = N$

$$\nu = \nu_o + (\bar{B}' - \bar{B}'')N^2 + (5\bar{B}' - \bar{B}'')N + 6\bar{B}' + \nu_k \qquad (8.30)$$

These equations illustrate the fact that in the absence of the spin orbit correction terms, five branches can be present in the rotational structure, which have the form of O, P, Q, R and S branches for the limiting case of a symmetric top; the correlation between the nomenclature and that in equations (8.22) to (8.30) is

O = P_1

P = Q_1 and P_2

Q = R_1, Q_2 and P_3

R = R_2 and Q_3

S = R_3

When the spin-orbit correction terms in equations (8.18) to (8.20) are included in the term values for the triplet state, the above coincidences are removed and in general, the full nine branches can occur for each (K' K") transition.

CHAPTER 9

ROTATIONAL ANALYSIS OF THE $^3A'' \leftarrow {}^1A'$ TRANSITION

I. ROTATIONAL ANALYSIS OF THE (0-0) BAND NEGLECTING N.S COUPLING:

The upper portion of Figure 16 reproduces the microdensitometer profile of the rotational structure of the (0-0) band of the $^3A'' \leftarrow {}^1A'$ transition in propynal. This was photographed in the first order of the Ebert Spectrograph, using a path length of 60 meters, and a pressure of 5 mm. Hg. for the absorbing gas as explained in Chapter 5. At the long wave length side of the central intensity maximum, which occurs at 4144 $\mathring{A}$, are a series of heads labelled K_3, K_4, K_5, ... which extend to the red with increasing separation between successive heads. A complex structure with little apparent regularity appears between the heads, and at the short wave length side of the band centre. Only an approximate analysis can be given for the rotational structure in this band, since individual rotational lines could not be completely resolved.

The wavenumbers for the centres of the K heads for HC≡CCHO and DC≡CCHO are collected in Table 10. It is possible to fit these to the equation

$$\nu = \nu_o + \text{const.} \times K^2 \qquad (9.1)$$

for values of K between 3 and 15. It then follows, from equation (8.16) that the sub-bands form part of the K structure arising from a

TABLE 10

WAVENUMBERS AND ASSIGNMENT OF THE K SUB-BAND MAXIMA

IN HC≡CCHO AND DC≡CCHO

K"	HC≡CCHO	DC≡CCHO
3	24,123.35	24,147.97
4	24,120.39	24,145.04
5	24,116.67	24,141.32
6	24,112.10	24,136.85
7	24,106.80	24,131.42
8	24,100.65	24,125.35
9	24,093.56	24,118.40
10	24,085.85	24,110.64
11	24,077.19	24,102.12
12	24,067.87	24,092.91
13	24,057.72	24,082.87
14	24,076.74	24,072.10
15	24,034.98	24,060.61

transition directed parallel to the axis; the molecule approximates to a near-prolate symmetric top not only in the ground but also in the excited electronic state. The observed polarisation confirms the predictions given in Chapter 5 that a mixing by spin-orbital interaction of the $^3A''$ with $^1A'$ state is primarily responsible for the transition. Since the separation between the adjacent sub-bands increases as the wavenumber decreases, it follows that

$$(A' - \bar{B}') < (A'' - \bar{B}'') \qquad (9.2)$$

The maxima assigned to the K sub-structure result from the superposition of many closely spaced rotational lines, and may be either unresolved Q branches, or heads in the other branches. If head formation is responsible for these peaks, their positions would not be expected to persist with such small deviations from the value calculated by equation (9.1) when extended to low values of K. Hence, these peaks are most probably unresolved Q branches.

If rotational distortion is neglected, the difference in wavenumber between the origin of the K sub-bands and the origin of the (K + 1) sub-band is

$$\Delta\nu_k = \left[(A' - \bar{B}') - (A'' - \bar{B}'')\right](K^2-(K+1)^2) =$$
$$- 2\left[(A' - \bar{B}') - (A'' - \bar{B}'')\right](K+1/2) \qquad (9.3)$$

The plot of the separations of the origins $\Delta\nu_k$ as a function of K is therefore a straight line. If (A'' - B'') is known, then (A' - B') can be obtained from the gradient. The straight line should intersect the K axis at K = -1/2.

Curvature of the line may be caused by non-rigidity of the rotating molecule. It follws from equation (8.9) that the correction

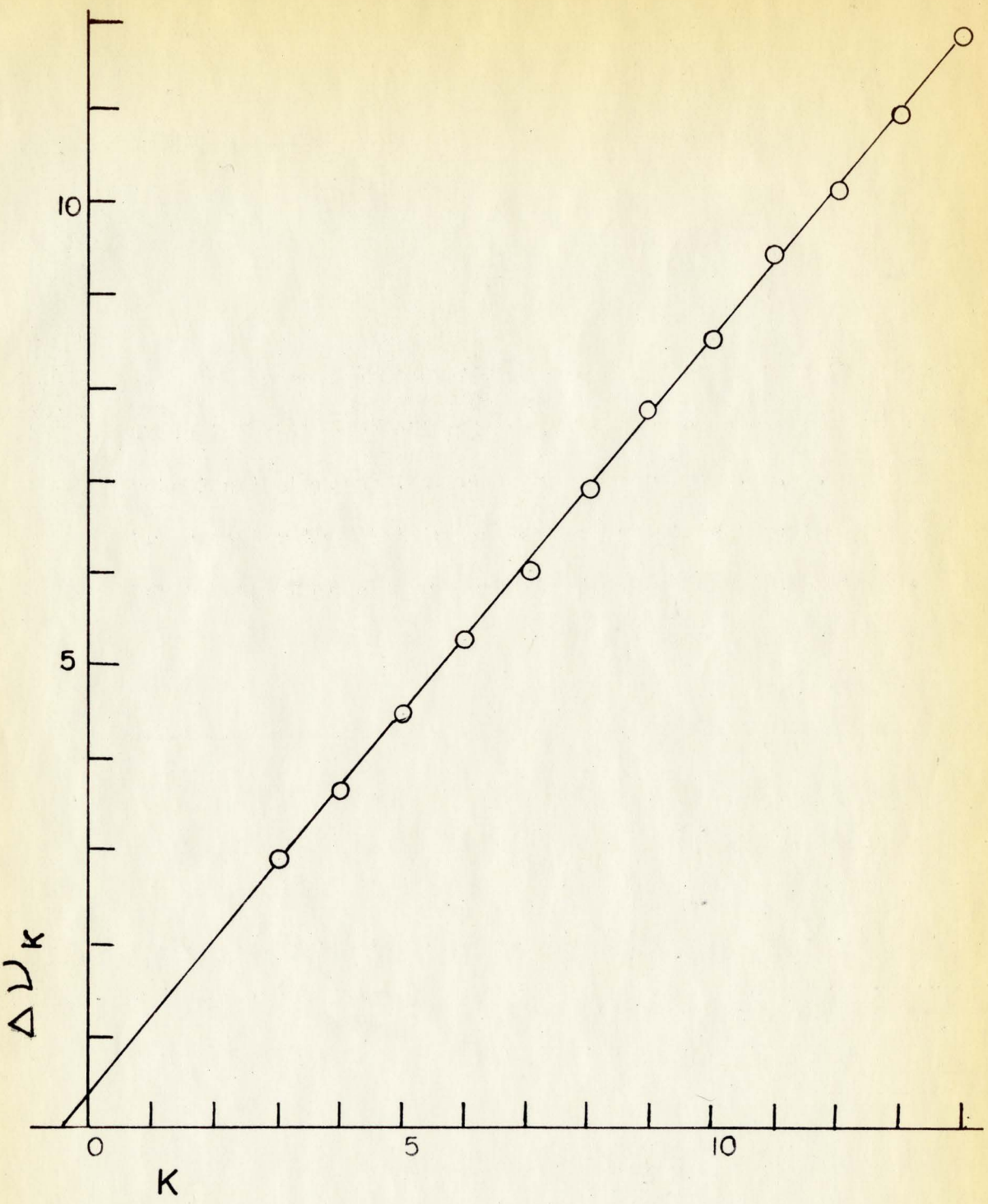

FIG.14 PLOT OF $\Delta\nu_K$ vs K

that must be added to equation (9.3) is equal to

$$(D'_k - D''_k)\left[(K+1)^4 - K^4\right] = (D'_k - D''_k)(4K^3+6K^2+K+1) \qquad (9.4)$$

and if $4K^3 > 6K^2+K+1$, the expression reduces to

$$(D'_k - D''_k) \times (4K^3) \qquad (9.5)$$

The plot of the separation of the centres of Q branches against K for the origin bands is shown in Figure 14 for HC≡CCHO. This is linear over the range K = 3 to K = 15, hence clearly showing that the rotational distortion is negligibly small. Deviation of the plot from linearity is considerably less than 1 cm^{-1} at K" = 15, so that according to equation (9.5), $|D'_k - D''_k| < 8 \times 10^{-5}$ cm^{-1}.

Figure 14 also shows that the K" numbering of the heads in Table 10 is correct, since when the line is extrapolated it intersects the K axis at a value close to $K = -\frac{1}{2}$, in agreement with equation (9.3) From the slope of this plot for HC≡CCHO and DC≡CCHO the approximate values are obtained in accordance with equation (9.3).

$$\text{HC}\equiv\text{CCHO} \quad (A' - \bar{B}') - (A'' - \bar{B}'') = -0.408 \text{ cm}^{-1} \qquad (9.6)$$

$$\text{DC}\equiv\text{CCHO} \quad (A' - \bar{B}') - (A'' - \bar{B}'') = -0.402 \text{ cm}^{-1}$$

More accurate values for these differences were obtained by fitting the wavenumbers of the heads in Table 10 to equation (8.16) by a least squares treatment. This yielded the values

$$\text{HC}\equiv\text{CCHO} \quad \nu = (24,126.86) \pm 0.12) - (0.4090 \pm 0.0017)K^2 \text{ cm}^{-1} \qquad (9.7)$$

$$\text{DC}\equiv\text{CCHO} \quad \nu = (24,151.12) \pm 0.14) - (0.4039 \pm 0.0014)K^2 \text{ cm}^{-1}$$

Since the values of the rotational constants in the ground state are known from the microwave studies[2], these equations give the excited

state values

$$HC{\equiv}CCHO \quad (A' - \bar{B}') = 1.7046 \quad cm^{-1} \qquad (9.8)$$

$$DC{\equiv}CCHO \quad (A' - \bar{B}') = 1.6790 \quad cm^{-1}$$

Accurate values for $\bar{B}'$ are difficult to obtain, since they must come from an analysis of the closely-spaced and incompletely resolved fine structure that constitutes the sub-bands. Unfortunately, no theoretical investigation has yet been made of the relative intensity factors for the rotational lines of a singlet-triplet transition in an asymmetric top, and so it is not possible to predict which of the rotational branches, equations (8.22) to (8.30), appear prominently in the spectrum. However, in their rotational analysis of the corresponding (0-0) band in the singlet-triplet system of formaldehyde, which has the same polarisation as the (0-0) band under investigation here for propynal, Robinson and DiGiorgio[27] found that only the P_1, R_1, P_3 and R_3 branches appeared strongly. It is reasonable to assume that the same branches will be observable in the case of propynal; the predictions in Chapter 5 indicate that only transitions to two of the spin components of the triplet state should appear strongly, as in the case of formaldehyde. In the latter molecule, the R_1 and P_3 branches were not separately resolved, and appeared as a single Q-type branch, which we here identify as responsible for the peaks that generate the K structure. The other predicted branches, P_1 and R_3, should have the appearance of O- and S-type branches respectively.

Since the Q branch in each observed sub-band is degraded to higher wavenumbers, we can expect that $\bar{B}' > \bar{B}''$, and therefore head formation only occurs in the $O(=P_1)$ branch. We assume here that spin-orbit interactions are relatively small, and no evidence to the contrary appears in the spectrum. The condition for head formation is $d\nu/dN=0$, and when this is applied to equation (8.22), the rotational constant for the upper state is obtained as

$$\bar{B}' = \bar{B}''(2N_H + 1)/(2N_H - 3) \qquad (9.9)$$

where N_H is the value at the head. A study of the observed rotational intensity distribution leads to the expectation that if the heads occur at N_H 40, they should be detectable in the spectrum, whereas for larger values of N_H they should be too weak to be observed. No such heads are observed in the spectrum, and therefore it is possible to fix a rough upper limit to $\bar{B}'$. If the values $N_H = 40$ and $\bar{B}'' = 0.1555$ cm^{-1} (obtained from the known ground state geometry) are inserted into equation (9.9), the value $\bar{B}' = 0.1636$ cm^{-1} is obtained, so that the actual value of $\bar{B}'$ is expected to lie between this figure and the ground state value of 0.1555 cm^{-1}.

Figure 15 illustrates the manner in which a closer estimate for $\bar{B}'$ was obtained. It shows a portion of the rotational fine structure extending to lower wavenumbers from the K" = 10 Q-branch maximum, a region that also contains lines belonging to the K" = 11 and K" = 12 sub-bands. The fine structure is complex in appearance, but nevertheless does show a regular pattern of lines separated by approximately 4B, which is the spacing that would be expected between successive members of an O-type branch on the assumption B'=B".

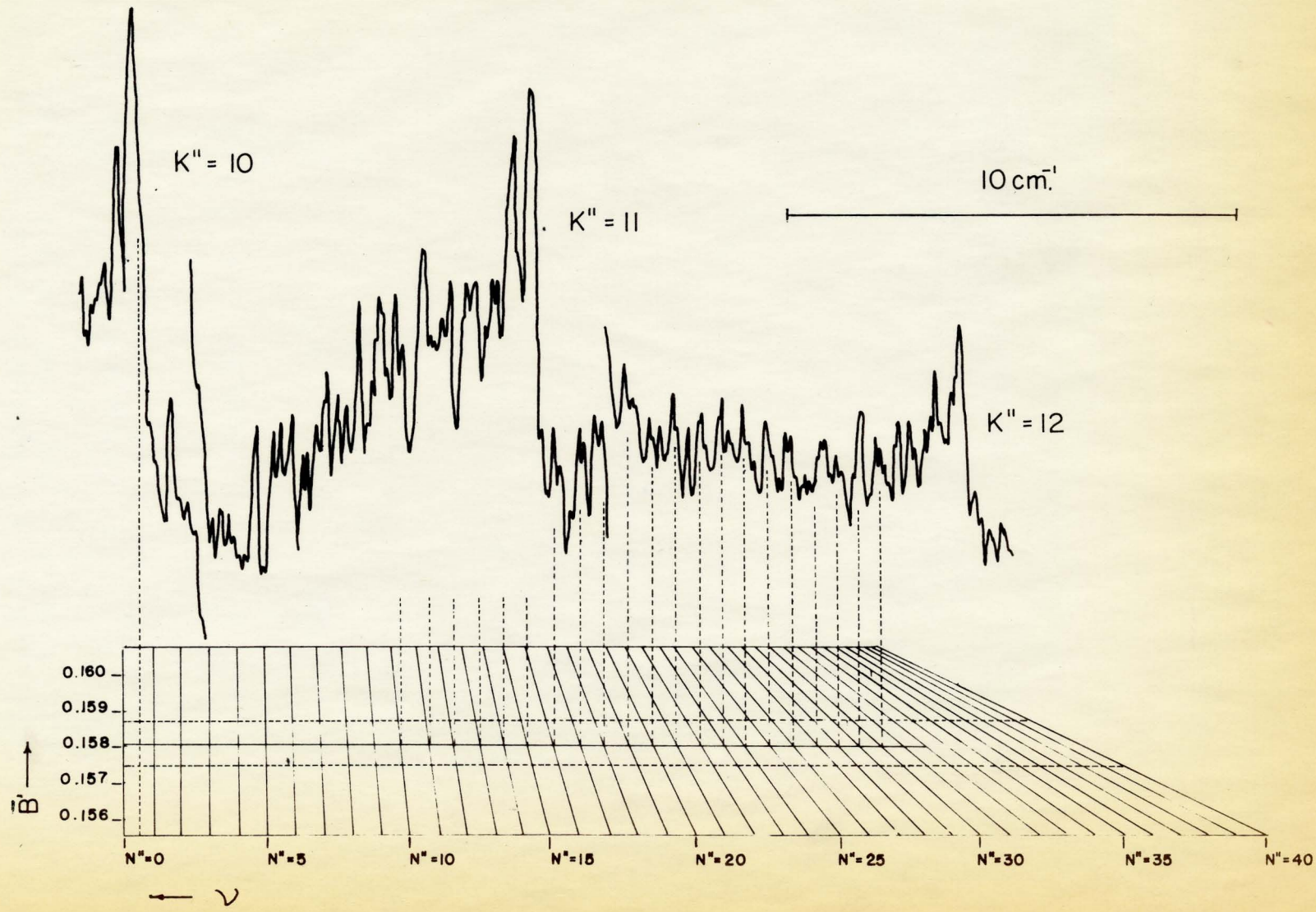

FIG. 15 DETERMINATION OF $\bar{B}'$

The wavenumbers in the lines of the P_1 branch in HC≡CCHO were calculated for the range of possible values for $\bar{B}'$ and the family of curves for N" = 0 - 40 were plotted as shown at the bottom of Figure 15. These were positioned so that the N" = 0 line coincided with the high wavenumber edge of one of the Q branch maxima, in this case having K" = 10; and vertical dotted lines originating upon the suspected O branch rotational lines were found to intersect the family of curves fairly consistently at the value $\bar{B}' = 0.1581 \pm 0.0007\ cm^{-1}$. We may therefore accept this value with some confidence, although it is impossible to achieve complete certainty under the spectral resolving power which could be achieved. A misassignment in the numbering of N by ± 1, that could result from uncertainty in the position of the sub-band origin, would only introduce an error of $\pm 0.0002\ cm^{-1}$ in the value of $\bar{B}'$.

A similar determination for DC≡CCHO yielded the value $\bar{B}' = 0.1466 \pm 0.0008\ cm^{-1}$.

When the moments of inertia for a planar asymmetric top molecule are determined from the measured rotational constants for a vibronic band, then there always exists a small inertial defect Δ in the relation

$$I_c - I_b = I_a + \Delta \qquad (amu\mathring{A}^2) \qquad (9.10)$$

is usually quite small; in the ground state of HC≡CCHO, $I_a = 7.4313$ $I_b = 104.7467$, $I_c = 112.3499$ and $\Delta = 0.1718$. If we assume that propynal is planar, or almost planar, in the excited state and that

Δ can be ignored, then the asymmetric top rotational constants B' and C' can be calculated from the formulae

$$B' = -(A' - \bar{B}') + (A'^2 + \bar{B}^2)^{\frac{1}{2}} \qquad (9.11)$$

$$C' = (A' + \bar{B}') - (A'^2 + \bar{B}^2)^{\frac{1}{2}}$$

When the values of $A' - \bar{B}'$ (9.18) and of $\bar{B}'$ given above are inserted in these equations, we obtain

	HC≡CCHO	DC≡CCHO	
A'	1.863	1.825	cm^{-1}
B'	0.1649	0.1525	cm^{-1}
C'	0.1513	0.1408	cm^{-1}

The rotational energy levels for the two combining electronic states were calculated in asymmetric rigid rotor approximation by the method of Bennett, Ross and Wells[28] on a Bendix G-15D computer. The computer was programmed to calculate all the rotational term values from the rotational constants for values of N ranging from 1 - 30. The positions of the rotational lines in cm^{-1} were then obtained as the differences between the term values in the ground and excited states, using the asymmetric rotor selection rules for a transition polarised along the a axis, together with the selection rule $\Delta N = 0, \pm 2$ that generates the O, Q and S branches. The O and S branches were presumed to have the same relative intensities as in formaldehyde and the intensity of the lines in each branch to reach a maximum at N = 20 and to be negligibly small at N = 40, in accordance with the relative thermal populations of the ground state levels. The decrease in intensity of the rotational lines comprising each sub-band as K"

increases was estimated from the intensities of the observed Q branch maxima. The resultant calculated spectrum is shown in Figure 16.

The assumptions that it was necessary to make about line intensities, in the absence of theoretical values, are fairly crude. However, in any case, it is difficult to evaluate the integrating effect of the finite slit width of the spectrograph upon the rotational lines, and so a close agreement between the observed and calculated spectra cannot be expected. With these reservations, it is seen that the two spectra are in fairly good agreement. The intensity maxima appear in approximately the same positions; at the (K" = 0) band origin, a large number of strong lines appear in the calculated spectrum which are unresolved in the central maximum of the observed structure. The strong line appearing midway between the observed K" = 6 and K" = 7 maxima is very likely caused by head formation in a branch originating at K" = 1 that is seen to be converging to lower wavenumbers. No intensity maxima are calculated to appear on the high wavenumber side of the central maximum, and none are indeed apparent in the spectrum.

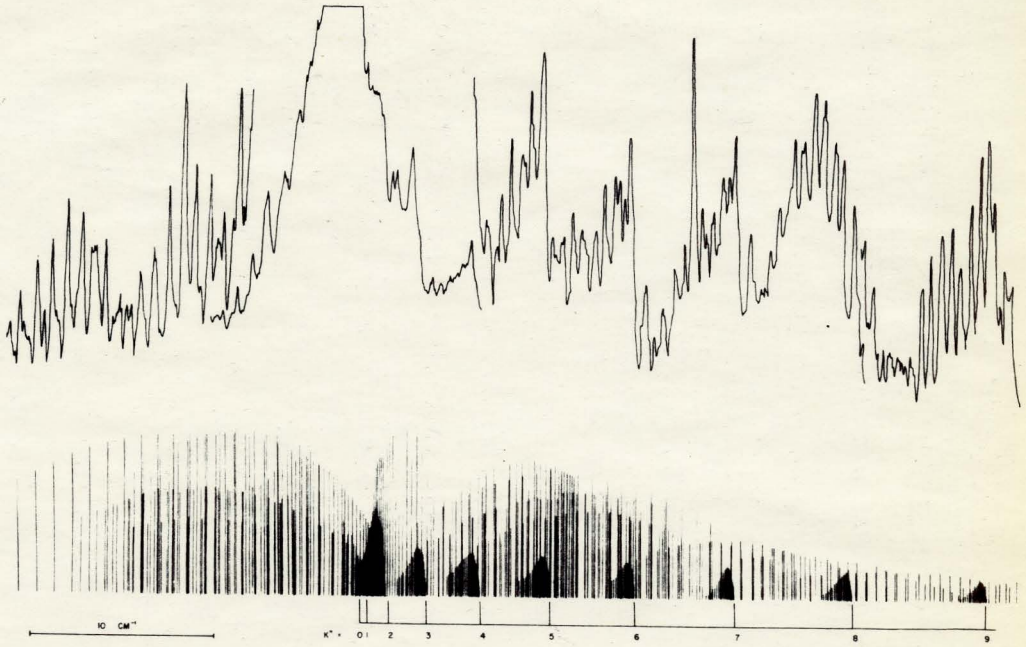

FIG.16 THE OBSERVED & CALCULATED BAND CONTOURS OF THE (0-0) BAND OF HC≡CCHO

CHAPTER 10

CONCLUSION

On the experimental side, the limiting factor that determined the depth of this study was the availability of isotopic forms of propynal in sufficient quantity and purity, since the material polymerised at room temperature and this process was accelerated by the action of visible and ultraviolet light. The infra-red spectrum was determined for the three species HC≡CCHO, DC≡CCHO and HC≡CCDO, but only the Raman spectrum of liquid HC≡CCHO was obtained. The production of the singlet-triplet emission spectrum consumed large quantities of propynal and was necessarily restricted to only the species HC≡CCHO. The low resolution absorption spectrum studies were also confined to this molecule, the DC≡CCHO samples being reserved for obtaining high resolution absorption spectra of the (0-0) origin band. The species HC≡CCDO was not available in sufficient quantity to fill the multiple reflection cell that was used to detect the weak singlet-triplet absorption bands. Synthesis of this species was not attempted, since the commercial firm from whom our sample originated informed us that the preparation has proved extremely difficult even for their skilled organic chemists.

The analysis of the infra-red and Raman spectra provided a satisfactory basis for analysing the emission spectrum of propynal. Comparison of this with the absorption spectrum of the singlet-triplet

system enabled the origin band to be determined and a reasonably satisfactory rotational analysis of this band has been carried out. This analysis shows that the observed polarisation of the band agrees with that predicted from theory for a $^3A'' \leftarrow {}^1A'$ electronic transition, and is different to that observed for the (0-0) band in the corresponding singlet-singlet transition. Transitions to only two of the three components of the excited state are apparent in the spectrum under high resolution, in agreement with the observations that have been made in the corresponding transition in formaldehyde. Spin-orbit interactions are relatively small in the triplet state of propynal, and their effects could not be detected in the spectrum. Although it was not possible to determine sufficient parameters for the geometry of the upper state to be calculated, the molecule remains a near-prolate asymmetric top ($\kappa = -0.984$) in the triplet state. The $n \longrightarrow \pi^*$ transition must be largely confined to the carbonyl group, and in a first approximation we may assume that only this group undergoes changes in geometry upon the electronic promotion. Let us accept the value of 0.1 Å for the increment in r(C=O), which has the value 1.215 Å in the ground state upon excitation.[3] This is the value for the extension in the singlet excited state obtained from calculations on the intensity distribution of the ν'_4 progression, and is close to the extension of 0.092 Å accompanying the singlet-triplet excitation of formaldehyde[27]. It is then possible to calculate from our rotational constants that the CCO angle decreases from the ground state value of 123° by approximately 4° in

the triplet state of propynal, assuming that the remaining geometry of the molecule is unchanged. However, it is quite likely that the molecule is, like formaldehyde, non-planar in the excited state .

BIBLIOGRAPHY

1. J. A. Howe and J. H. Goldstein, J.Chem.Phys.23,1223 (1955).
2. C. C. Costain and J. R. Morton, J.Chem.Phys.31,389 (1959).
3. J. A. Howe and J. H. Goldstein, J.Am.Chem.Soc.80,4846 (1958).
4. F. Willie and L. Saffer, Ann.Chem.Liebigs 568,34 (1950).
5. N. J. Leonard, Editor, Organic Syntheses, 36,66 (1956).
6. J. T. Edsall and E. B. Wilson, J.Chem.Phys.6,124 (1938).
7. J. C. Evans, J.Chem.Phys. 22, 1228 (1954).
8. J. K. Wilmshurst, J.Mol.Spectrosc. 1, 201 (1957).
9. R. A. Nyquist and W. J. Potts, Spectrochim.Acta 16,419 (1960)
10. G. C. Pimental and A. L. McClellan, The Hydrogen Bond. W. H. Freeman, San Francisco (1960).
11. J. R. Platt, J.Chem.Phys.19,101 (1951).
12. S. F. Mason, Quart.Rev.15,287 (1961).
13. V. G. Krishna and L. Goodman, J.Chem.Phys.36,2217 (1962)
14. J. W. Sidman, J.Chem.Phys.29,644 (1958).
15. J. U. White, J.Opt.Soc.Am. 32,285 (1942).
16. B. Edlen, J.Opt.Soc.Am. 43,339 (1953).
17. G. W. King, J.Sci.Instr.35,11 (1958)
18. G. R. Harrison. MIT Wavelength Tables. Wiley, New York (1939).
19. J. H. Callomon, Proc.Roy.Soc.A 244,220 (1958).
20. R. W. B. Pearse and A. G. Gaydon, The Identification of Molecular Spectra. Chapman and Hall, London (1950).
21. J. C. D. Brand, J. H. Callomon and J. K. G. Watson, Can.J. Phys.39, 1508 (1961)

22. J. O.Hirschfelder, J.Chem.Phys. 8,431 (1940).

23. G. Herzberg, Infrared and Raman Spectra of Polyatomic Molecules. Van Nostrand, New York (1945).

24. R. S. Henderson and J. H. Van Vleck, Phys.Rev.74,106 (1948).

25. R. S. Henderson, Phys.Rev.100,723 (1955).

26. G. W. Robinson and V. E. DiGiorgio, Can.J.Chem.36,31 (1958).

27. V.E. DiGiorgio and G. W. Robinson, J.Chem.Phys.31,1678 (1959).

28. J. M. Bennett, I. G. Ross and E. J. Wells, J.Mol.Spectrosc. 4,342 (1960)